



ACTA PATHOLOGICA, MICROBIOLOGICA ET IMMUNOLOGICA SCANDINAVICA

Volume 126 Supplement 141 April 2021

Implant-associated osteomyelitis: Development, characterisation, and application of a porcine model

Louise Kruse Jensen

Department of Veterinary and Animal Sciences, Faculty of Health and Medical Science, University of Copenhagen, Copenhagen, Denmark

The Faculty of Health and Medical Sciences at the University of Copenhagen has accepted this dissertation for public defence for the doctoral degree in medicine.

Copenhagen, 27 January 2021.

Dean Ulla Wever, Head of Faculty

The defence is conducted as a digital defence with partly physical presence on Friday 4th of June 2021 at 01:00 pm.

WILEY

PREFACE

The author would like to thank the Independent Research Fund Denmark (Technology and Production) and the EU Horizon 2020 research programme for funding the research presented in this doctoral dissertation.

In particular, I would like to thank Professor in Veterinary Pathology Henrik Elvang Jensen who participated in all parts of the experimental studies. Thanks for your inspiration, guidance and enthusiasm. My thanks also go to all the staff at the Pathobiological Sciences Section for being great colleagues and for the many happy times during work and social events. A special thanks to laboratory technicians Elizabeth Petersen and Betina Andersen for all your help in the histo-lab. I apologise for all the challenging and problematic issues regarding histological preparation of bones. Many thanks also to technicians Dennis Brok and Frederik Andersen for their skilful technical support and help producing images. I would also like to thank the animal technicians at the Department of Experimental Medicine for their excellent care of the pigs and help with anaesthesia, blood sampling and inoculation procedures.

Thank you to all my research assistants during the past 5 years, including Kristine Dich-Jørgensen, Anne Sofie Boym Johansen, Nicole Lind Henriksen and Amalie Blirup-Plum. Thank you for your hard work, including endless hours spent evaluating and scoring histological slides, and thank you for bringing enthusiasm and fun into our daily routine.

Thanks also to Expert in Experimental Surgery Janne Koch, Associate Professor in Veterinary Microbiology Bent Aalbæk and to Professor in Chronic Infections and Biofilm Thomas Bjarnsholt. You have all been indispensable for the research described in this dissertation. Thomas, I enjoyed our biofilm discussions and I am grateful for all your support.

Thanks to everyone in Professor and Orthopedic Surgeon Kjeld Søballe's research group at Aarhus University Hospital for our collaboration on antimicrobial penetration into infected bone tissue. Mikkel Tøttrup, Pelle Hanberg and Mats Bue, it has been a pleasure to work with you.

Finally, thanks to all my friends and family for their never ending support and trust, and thanks to my wonderful husband and daughters, Kim, Alberte and Frida, for your love and patience.

Contents

TITLE PAGE	1	Time frame	19
PREFACE	2	Post-mortem quantification of bone infection	20
CONTENT	3	CT-scanning	20
BASIS OF THE DISSERTATION	4	Macroscopic pathology	20
SUMMARY	5	Histopathology	20
SUMMARY IN DANISH (RESUME)	6	Microbiology	24
INTRODUCTION	7	Embolic spread from the local bone infection	25
OVERVIEW OF DISSERTATION	8	Comparison with previous porcine bone infection models	25
CHAPTER 1 IMPLANT-ASSOCIATED OSTEOMYELITIS (IAO)	8	Comparison with IAO in humans	25
Classification of IAO	8	CHAPTER 4 APPLICATION OF THE PORCINE IAO MODEL – TISSUE BIOFILM	27
Pathology of IAO	9	In vivo biofilm	27
Aetiology and pathogenesis of IAO	10	Porcine models of biofilm infections in humans	27
Biofilm in IAO	10	Tissue biofilm	28
CHAPTER 2 ANIMAL MODELS OF BONE INFECTIONS	11	New staining technique for Staphylococcus aureus tissue biofilm	29
Non-rodent animal models of bone infections	11	Sampling of tissue	30
Findings related to study design	12	Histochemistry and immunohistochemistry	30
Pathological remarks	12	CHAPTER 5 APPLICATION OF THE PORCINE IAO MODEL – ANTIMICROBIAL AGENTS	32
Microbiological remarks	13	Treatment of IAO	32
Methodological quality	14	Antimicrobial pharmacokinetics in infected bone tissue	33
Standard study template guidelines	14	Histopathology associated with reduced antimicrobial penetration	35
Modelling of bone infections in pigs	14	Local antibiotic treatment of bone infections	36
The pig as an experimental animal	14	In vivo susceptibility to gentamicin	37
Osteological advantages	15	CHAPTER 6 CONCLUSIONS AND PERSPECTIVES	38
Immunological advantages	16	REFERENCES	38
CHAPTER 3 A PORCINE MODEL OF IMPLANT-ASSOCIATED OSTEOMYELITIS (IAO)	17		
Animals and inoculum	17		
Surgical inoculation procedure and perioperative period	18		

Basis of the dissertation

The publications on which this doctoral dissertation is based are referred to in the text by their roman numerals (I–IX):

- I: Tøttrup M, Bue M, Koch J, **Jensen LK**, Hanberg P, Aalbæk B, Fuursted K, Jensen HE, Søballe K. Effects of implant-associated osteomyelitis on cefuroxime bone pharmacokinetics: assessment in a porcine model. *J Bone Joint Surg Am* 98 (5): 363–369, 2016.
- II: **Jensen LK**, Koch J, Aalbæk B, Moodley A, Bjarnsholt T, Kragh KN, Petersen A, Jensen HE. Early implant-associated osteomyelitis results in a peri-implanted bacterial reservoir. *APMIS* 125 (1): 38–45, 2017.
- III: **Jensen LK**, Koch J, Dich-Jorgensen K, Aalbæk B, Petersen A, Fuursted K, Bjarnsholt T, Kragh KN, Tøttrup M, Bue M, Hanberg P, Søballe K, Heegaard PMH, Jensen HE. Novel porcine model of implant-associated osteomyelitis: a comprehensive analysis of local, regional, and systemic response. *J Orthop Res* 35 (10): 2211–2221, 2017.
- IV: **Jensen LK**, Johansen ASB, Jensen HE. Porcine models of biofilm infections with focus on pathomorphology. *Front Microbiol* 8 (article no. 1961): 1–15, 2017.
- V: **Jensen LK**, Koch J, Henriksen NL, Bue M, Tøttrup M, Hanberg P, Søballe K, Jensen HE. Suppurative inflammation and local tissue destruction reduce the penetration of cefuroxime to infected bone implant cavities. *J Comp Pathol* 157 (4): 308–316, 2017.
- VI: **Jensen LK**, Henriksen NL, Bjarnsholt T, Kragh KN, Jensen HE. Combined staining techniques for demonstration of *Staphylococcus aureus* biofilm in routine histopathology. *J Bone Jt Infect* 3 (1): 27–36, 2018.
- VII: Bue M, Hanberg P, Koch J, **Jensen LK**, Lundorff M, Aalbæk B, Jensen HE, Søballe K, Tøttrup M. Single-dose bone pharmacokinetics of vancomycin in a porcine implant-associated osteomyelitis model. *J Orthop Res* 36 (4): 1093–1098, 2018.
- VIII: **Jensen LK**, Bjarnsholt T, Kragh KN, Aalbæk B, Henriksen NL, Blirup SA, Pankoke K, Petersen A, Jensen HE. In-vivo gentamicin susceptibility test for prevention of bacterial biofilms in bone tissue and on implants. *Antimicrob Agents Chemother* 63: 1–10, 2019.
- IX: **Jensen LK**, Henriksen NL, Blirup SA, Jensen HE. Guideline for preclinical studies of bone infections in large animals based on a systematic review of 316 non-rodent models. *J Bone Joint Surg Am* 101 (21): 1894–1903, 2019.

Summary

Worldwide, there has been an ongoing increase in the number of bone infections that lead to amputations and lifelong disability, affecting millions of people every year. Therefore, research investigating the prevention, diagnosis and treatment of bone infections is vitally important. However, to develop effective new approaches and techniques for managing bone infections, preclinical testing and evaluations using reliable animal models are necessary. A novel porcine model of implant-associated osteomyelitis (IAO) in humans was recently developed. The model was based on female pigs, and osteomyelitis was induced by inoculation of *Staphylococcus aureus* bacteria into a pre-drilled tibial cavity (2 x 20 mm). Following inoculation, a steel implant (2 x 15 mm) was inserted into the cavity. The animals were euthanized 5 days after inoculation. Control pigs were exposed to the same surgical procedure and inoculated with sterile saline. The success rate of the model was 100%, i.e., all the pigs inoculated with bacteria developed osteomyelitis. Bone lesions similar to those found in human patients with osteomyelitis developed in the porcine IAO model, and the inoculated bacteria were detected both within peri-implant bone tissue and on the surface of the implants. Thus, peri-implant bone tissue may serve as a reservoir for biofilm (bacterial aggregates surrounded by an extracellular matrix) shortly after surgical contamination. Biofilms are extremely tolerant to antibiotics and are reportedly the main reason for human bone infection treatment failure. This new porcine IAO model was used to develop a biofilm staining technique, which combined histochemistry (HC) and immunohistochemistry (IHC). The new staining technique allowed the bacterial cells and extracellular matrix to be visualised simultaneously: Alcian blue pH3 stained the carbohydrates of the extracellular matrix blue, and IHC treatment with an antibody specific for *S. aureus* coloured the bacterial cells red. The new staining technique could also be used reliably on human bone tissue with chronic staphylococcal osteomyelitis.

Two microdialysis studies were performed using the porcine IAO model. These studies found that systemically administered antibiotics (cefuroxime and vancomycin) showed significantly less penetration into the tissue surrounding infected bone implants than into healthy bone tissue. Furthermore, this reduced antimicrobial penetration was correlated with the progression of peri-implant bone lesions. Bone lesions that extended to a depth of > 3 mm from the implant cavity into the bone tissue showed almost no antimicrobial penetration. The reduced penetration was due to suppurative and necrotic bone inflammation and expansion of the implant cavity. Consequently, diffusion of antimicrobial agents from the capillary system into the implant cavity was hampered because it had to cover a greater distance. Bone inflammation also had a negative impact on the efficacy of a single dose of locally administered gentamicin. Different doses of gentamicin were added to the inoculum 1 min prior to inoculation into the porcine IAO model. Due to the development of acute inflammation including vasodilatation and increased vascular permeability, only high doses of gentamicin (>1000 minimum inhibitory concentration) were effective at the implant surface. This shows that the prophylactic concentration of locally administered antimicrobial agents cannot be evaluated solely by using *in vitro* assays.

A systematic review of all contemporary large, non-rodent animal models of bone infection (i.e., goats, sheep, dogs, pigs and rabbits) was performed. Overall, it was found that experimental design was poorly reported, methods were of poor quality and the pathological parameters used varied significantly. Therefore, study template guidelines as a standard for reporting on animal models of bone infection was established. It was apparent that the animal species per se was one of the most important study design parameters. Based on a narrative review, we found that there were many advantages in using pigs for modelling bacterial biofilm infections in humans because comparable infections also occur spontaneously in pigs.

Currently, there are many problems associated with treating patients who have chronic biofilm-based infections, including bone infections. Furthermore, the increasing prevalence of antimicrobial resistance means that new treatments for infectious diseases are urgently required. The novel porcine IAO model described here is a valuable and reliable tool for investigating new prophylactic strategies and treatment regimens for bone infections in humans.

Summary in Danish (resume)

Flere og flere patienter får diagnosen knogleinfektion. En knogleinfektion fører til operation, indlæggelse, flere ugers antibiotikabehandling og i yderste konsekvens amputation. De fleste knogleinfektioner opstår, fordi der kommer bakterier ind i knoglen under en operation. Det kan være under indsættelsen af en ny kunstig hofte, eller ved korrektion af et benbrud hvor der anvendes osteosyntese. Knogleinfektioner er enormt svære at behandle, fordi bakterierne danner biofilm, dvs. de går i dvale, og danner en beskyttende matrix omkring sig. Biofilmdannelse beskytter bakterierne mod kroppens eget immunforsvar og det antibiotikum som gives i behandlingsøjemed. Den stigende udvikling af antibiotikaresistens udgør en alvorlig trussel mod vores evne til at bekæmpe infektioner, og derfor er forskning indenfor forebyggelse, diagnosticering og behandling af knogleinfektioner mere relevant end nogensinde før. For at udvikle nye tiltag og teknikker med klinisk relevans, er det helt afgørende, at disse testes og evalueres i velkarakteriserede dyremodeller, som efterligner den humane patologi. Denne afhandling beskriver udviklingen, karakteriseringen og anvendeligheden af en ny grisemodel for implantat-relateret osteomyelitis hos mennesker.

Grisemodellen er baseret på, at der bores en lille kavitet i højre tibia hvori der inokuleres saltvand eller *Stafylokokkus aureus* bakterier. Efter inokuleringen indsættes et lille implantat (2x15mm). Grisene aflives efter 5 dage og alle dyr inokuleret med bakterier udvikler komparative knoglelæsioner. De inokulerede bakterier genfindes på både det indsatte implantat og et stykke inde (1 cm) i det omgivende væv. Modellen demonstrerer dermed, at det knoglevæv som omgiver et implantat kan udgøre et biofilmreservoir allerede kort tid efter kirurgisk kontaminering. Den nye grisemodel er blevet brugt til, at udvikle en ny farvemethode der kan synliggøre biofilmdannelse i vævsnit ved brug af almindelig lysmikroskopi. Princippet i den nye metode er en kombination af almindelig histokemi og immunohistokemi. Ved at kombinere en protokol for Alcian Blue pH3 med immunhistokemi baseret på et *S. aureus* specifikt antistof, kunne både matrix og bakterier i biofilmaggregater visualiseres i to forskellige farver. Den nye farvemethode er også anvendt på humant væv med kronisk osteomyelitis.

Knogleinfektioner kræver lang tids antibiotikabehandling og de eksisterende doseringsprotokoller bygger på farmakokinetiske studier af rask knoglevæv. Baseret på grisemodellen for implantat-relateret osteomyelitis blev det demonstreret, at penetrationen af systemisk indgivet antibiotika (cefuroxime og vancomycine) til inficerede knogleimplantater, er signifikant reduceret sammenlignet med normalt rask knoglevæv. Den reducerede antibiotika penetration var korreleret til udbredelsen af patologiske forandringer i knoglevævet omkring implantatet. I de tilfælde hvor læsionerne udbredte sig mere end 3 mm fra implantatet, var der næsten ingen penetration. Den reducerede penetration blev forårsaget af en purulent og nekrotisk inflammation, hvilket ødelagte knoglevævet og skabte en kavitet omkring implantat. Derfor kan det antages, at diffusion af antibiotika fra kapillærerne og indtil implantatet er blevet nedsat delvist pga. en øget diffusionsafstand. Udover den store effekt på penetrationen af antibiotika, blev det også påvist, at det inflammatoriske respons har stor indflydelse på effekten af lokal indgivet antibiotika. Forskellige doser af gentamicin blev iblandet det bakterielle inokulum et minut før inokulering i grisemodellen. På grund af udviklingen af akut inflammation, med vasodilation og øget vaskulær permeabilitet, var det kun de meget høje gentamicin doser (>1000 MIC) som kunne fastholde en baktericid koncentration på implantatets overflade. Derfor kan det konkluderes, at det for knogleinfektioner, er utilstrækkeligt at basere effekten af antibiotika udelukkende på studier af rask væv og på *in vitro* assays.

I et stort systematisk review af alle ikke-gnaver modeller for knogleinfektioner blev det påvist, at der de sidste 10 år er sket en markant stigning i brugen af større forsøgsdyr som fx får og grise. Det blev også påvist, at afrapporteringen af studiedesign ofte var meget mangelfuld, og at den metodologiske kvalitet var meget lav. Dette førte til udviklingen af et set retningslinjer for standard afrapportering ved udvikling og anvendelse af dyremodeller for knogleinfektioner. Det systematiske review viste, at dyrearten er en af de mest afgørende design parameter. Baseret på en gennemgang af alle grisemodeller for bakterielle infektioner hos mennesker, blev det konkluderet, at grisemodeller er særdeles fordelagtige som modeldyr for biofilm baseret infektioner hos mennesker, fordi grise (slagtesvin) udvikler komparative infektioner spontant.

Der er store problemer med behandlingen af patienter som lider af kroniske infektioner inklusive knogleinfektioner. Det er tydeligt, at den nye grisemodel for implantat-relateret osteomyelitis er et brugbart og pålideligt redskab, til at studere nye profylaktiske strategier og behandlingsregimer.



Implant-associated osteomyelitis: Development, characterisation, and application of a porcine model

LOUISE KRUSE JENSEN

Department of Veterinary and Animal Sciences, Faculty of Health and Medical Science, University of Copenhagen, Copenhagen, Denmark

INTRODUCTION

Worldwide, there has been an ongoing increase in the number of bone infections that lead to amputations and lifelong disability, affecting millions of people every year [1,2]. Consequently, bone infections constitute a substantial economic burden in terms of patients, physicians, hospitals and healthcare systems [1,2]. When applied to patients, the term ‘bone infection’ can include prosthetic joint infections (PJIs), fracture-related infections (FRIs), implant-associated osteomyelitis (IAO), chronic osteomyelitis (CO), osteomyelitis in children and diabetic foot osteomyelitis (DFO) [3]. Presently, DFO is the leading cause of lower extremity amputations, and it is estimated that a lower limb is lost every 30 s due to DFO [4,5]. The increased number of bone infections is mainly due to an increase in the size of the elderly population, an increased prevalence of diabetes and an increase in the number of joint prostheses and bone fixation implants being used [1]. The persistence of the problem and the unsatisfactory proportion of positive treatment outcomes implies that the current prophylaxis and treatment strategies are incomplete despite best practice [2]. Therefore, future research must focus on prevention, diagnosis and treatment of bone infections. However, the development of effective new approaches and techniques will depend on preclinical testing and evaluations performed in reliable animal models. In this dissertation, a novel porcine IAO model is presented. The publications referred to (I–IX) describe the development, characterization and application of this model.

Chronic bacterial infections are generally caused by biofilm-forming bacteria [6].

Therefore, it is surprising that most reports regarding bacterial biofilms are based on *in vitro* observations, because these laboratory findings cannot be extrapolated into clinical settings (VIII) [7]. Consequently, there are many problems associated with treating patients who have chronic biofilm-based infections, including bone infections. In addition, the increasing prevalence of antimicrobial resistance means that new treatments for chronic infectious diseases are urgently required [8]. The porcine IAO model has generated new relevant *in vivo* observations regarding biofilms (II, VI, VIII). In particular, studies have shown that biofilms do not simply involve artificial surface attachment; therefore, the old dogma used to describe biofilms in terms of a ‘race for the surface’ seems to be clinically inadequate (II, VI, VIII). Biofilm formation also affects tissues, and research into both tissue and implant biofilms is equally important for evaluating chronic bone infections. Promising new approaches to prevent biofilm formation in orthopaedic research include the following: 1) modification of implant surfaces to prevent bacterial adhesion, 2) coating of implants so that they can elute high concentrations of antibiotics locally (without causing systemic toxicity), 3) new drugs directed against bacterial adhesion molecules or quorum sensing and 4) the development of vaccines against biofilm-forming bacteria [9]. All of these new technologies for combating osteomyelitis may be tested using the porcine IAO model.

During the past 5 years, the porcine IAO model has been applied in several studies [10–13]. In brief, the model was used as the basis of an EU HORIZON 2020 Research and

Innovation Programme project (Novel Marine Biomolecules Against Biofilm [NoMoRFilm] no. 634588) to identify new antibiotics in micro-algae. As a result, one promising anti-biofilm compound was isolated, synthesized, chemically characterized and evaluated for anti-infective properties in the porcine model. In addition, the NoMorFilm project also resulted in the development of a new surface-coating technique for orthopaedic implants. This technique provides a coating that can bind and release high concentrations of antibiotics. An EU patent application based on the new coating technique is currently under review and describes very successful test results obtained using the porcine IAO model. In addition to the prophylactic coating studies, the porcine model was also recently used to evaluate the therapeutic impact of a gentamicin-loaded biodegradable bone void filler, following limited or extensive debridement of osteomyelitis lesions [12]. Currently, the porcine IAO model is also being used to investigate the molecular orchestration of bacterial bone infections. Gene expression analyses of porcine and human infected bone biopsies have shown that bone tissue can mount and sustain a local acute phase response (i.e. an extra hepatic acute phase response) [11]. In addition, research has shown that the classical receptor activator of nuclear factor κ B (RANK)–RANK-ligand (RANKL) pathway is not responsible for bone loss resulting from bacterial osteomyelitis [13]. In particular, the molecular studies demonstrated upregulation of specific inflammatory genes, which had no murine homologues; that is, the corresponding genes are not present in mice.

OVERVIEW OF DISSERTATION

This dissertation consists of six chapters. Chapter 1 provides background information regarding IAO in humans. Chapter 2 focuses on previously studied non-rodent animal models of bone infections and the advantages of using pigs for modelling osteomyelitis. In Chapter 3, the development of the new porcine IAO model is described. Chapter 4 focuses on a new staining technique for *in situ* visualization of biofilms and biofilm formation in spontaneous porcine

bacterial infections. Chapter 5 describes the application of the porcine IAO model in studies investigating antimicrobial penetration into infected bone tissue and the prevention of biofilm formation. Finally, Chapter 6 summarizes the main conclusions from the publications on which this dissertation is based.

CHAPTER 1

Implant-associated osteomyelitis (IAO)

Classification of IAO – In elective trauma surgery, bone infections occur at a rate of 1%–5% after closed fractures, and at a rate of 3%–50% after open fractures [14]. In 2004, it was estimated that two million fracture fixation procedures were performed each year in the United States leading to approximately 100,000 cases of IAO annually [15]. Risk factors for the development of infections include smoking and comorbidities such as diabetes, immunosuppression and chronic infections at other sites [16]. Fractures occur most frequently in the feet and hands, followed by the long bones, that is the humerus, radius, ulna, femur, tibia and fibula (Fig. 1) [16]. If IAO occurs after fracture fixation of a long bone, this may delay healing (Fig. 1) or lead to permanent functional loss or even amputation of the affected limb [2,16].

The term ‘osteomyelitis’ refers to inflammation of the bone marrow, and the term ‘osteitis’ refers to inflammation of the entire bone including the cortex [14]. Commonly, osteomyelitis is the preferred term and this is used synonymously for both bone infection conditions in patients [14]. IAO may be classified based on the time from surgery to occurrence of the infection. ‘Early infections’ are seen within 2 weeks after bone fixation, ‘delayed infections’ between the third and the 10th week, and ‘late infections’ occur more than 10 weeks after implantation [2,16]. ‘Late infections’ can be acute if they are caused by a haematogenous infection; otherwise, they represent a chronic ‘delayed infection’ or the recurrence of an incorrectly treated ‘early infection’ [16]. Clinically, osteomyelitis is also frequently classified as either acute or chronic. CO is subjectively defined as a bone infection with symptoms that persist for at least



Fig. 1. Surgical treatment of IAO in a 68-year-old man. The infection was caused by *Staphylococcus epidermidis*. (A) Non-healing wound over the lower tibial bone. (B) Removal of infected osteosynthetic material during debridement of infected bone tissue. (C) Complete debridement showing pinpoint bleeding of vital cortical bone tissue. (D) A bone void filled with an antibiotic-eluting degradable biocomposite. The wound was closed using a free muscular flap.

6 weeks, the presence of bone pathology in an image, or infections that require major interventions due to sequestra or deformities [17]. In adults, CO is often associated with foreign bodies, for example implants [17]. Therefore, ‘delayed’ or ‘late’ IAO may also be characterized/described as CO.

Osteomyelitis in the long bones may also be classified using the Cierny–Mader staging system, which correlates with treatments and prognoses [18,19]. The terms ‘acute’ and ‘chronic’ are not used in this classification system and the stages are dynamic, reflecting the anatomy and pathophysiology of the disease [18,19]. The Cierny–Mader system classifies osteomyelitis into four stages [18,19]. Stage 1, or medullary, osteomyelitis is confined to the medullary cavity of the bone. Stage 2, or superficial, osteomyelitis involves only the cortical bone. Stage 3, or localized, osteomyelitis usually involves both cortical and medullary bone. In this stage, the bone remains stable, and the infection does not involve the entire bone diameter. Stage 4, or diffuse, osteomyelitis involves the entire diameter of the bone, with loss of stability. The Cierny–Mader system includes a second dimension and classifies the host as A, B, or C [18,19]. An A-host is a patient with no systemic or local compromising factors [18]. The B-host is affected by systemic or local factors that affect the immune

response, metabolism and local vascularity [18]. C-hosts are patients who are so severely compromised that they cannot have surgery [18].

According to McNally et al., the definition of IAO implies at least one of the following criteria: [16]

- Pus surrounding the implant.
- A sinus tract communicating with the implant
- Evidence of an identical microorganism in at least two samples (e.g. biopsies, exudate or sonication fluid).
- The presence of >5 neutrophil granulocytes (NGs) per 10 high-power fields (HPFs) in a biopsy.

Pathology of IAO – The presence of pyogenic bacteria within bone tissue and on the surface of bone implants will lead to a suppurative inflammatory reaction dominated by neutrophils (II, III, V) [17,19]. Bone lysis will be induced by proteolytic enzymes released from the inflammatory cells and the activation of matrix metalloproteinases [20]. Furthermore, the activation of osteoclasts will also contribute to bone matrix resorption [20]. Within the trabecular bone tissue, suppuration will increase the intraosseous pressure and cause compression of blood vessels resulting in thrombosis,

which leads to ischaemic bone necrosis (i.e. trabecular sequestra; II, III, V) [17,19]. If the exudate enters and spreads within the cortical Volkmann's and Haversian canals, this will lead to a compromised medullar and periosteal blood supply and generate separated dead cortical segments (i.e. sequestra) [17,19]. Regardless of location, a bone sequestra provide a perfect substrate for bacterial growth [17,19]. Eventually, an infectious bone lesion will contain granulation tissue and fibrosis, which may be surrounded by osteoid-producing osteoblasts [17,19]. Osteogenic stem cells in the periosteum will differentiate into osteoblasts and form a sheath of vital bone, called an involucrum, which surrounds the dead cortical bone [17,19]. The involucrum is irregular and is often perforated with openings through which pus may spread into the surrounding soft tissues and ultimately drain to the skin surface via a sinus tract. The density of the involucrum may gradually increase and eventually almost forms a new diaphysis [17,19].

Aetiology and pathogenesis of IAO – Most cases of IAO are caused by Staphylococci, and *Staphylococcus aureus* and *Staphylococcus epidermidis* (Fig. 1) are the most common aetiologies [2,16,21]. Other pathogens that are frequently responsible for IAO include Streptococci, coagulase-negative staphylococci, virulent gram-negative bacteria and *Propionibacterium acnes* [2,16,21]. Early infections are often caused by highly virulent pathogens such as *S. aureus*, Group A *Streptococcus* and gram-negative bacteria [2,16,21]. The three major routes by which bacterial pathogens can access bone tissue are: 1) direct, 2) haematogenous or 3) contiguous. [16] Direct or exogenous infections are caused by bacterial contamination of the bone tissue during trauma and surgery or during the perioperative period [16]. Haematogenous infections occur due to bacterial seeding following bacteraemia, and contiguous infections are a result of progression from arthritis or soft tissue infections to the adjacent bone fixation device [16].

Biofilm in IAO – Both bone tissue exposed to surgery and the inserted bone implants are highly susceptible to infections [19,22]. If the

infecting bacteria are not eliminated rapidly, they will adhere to the bone tissue and/or the surface of the implant (II, III, VI, VIII) [19,22]. This process of bacterial attachment is mediated by physical factors, for example surface tension, hydrophobicity and electrostatic interactions or specific adhesion to plasma proteins such as fibronectin and fibrin [22–24]. Normally, healthy bone tissue is highly resistant to infection. Thus, the increased susceptibility to infection is a direct consequence of orthopaedic procedures. Orthopaedic surgery to implant plates, screws or prostheses, correct fractures or debride IAO will cause tissue damage and bleeding of exposed bone ends (Figs 1C and 2B). Immediately thereafter, the bone tissue and any inserted implant will be covered by plasma proteins (Figs 2 and 3). Interestingly, the plasma protein coating plays a more important role in bacterial surface adhesion to implants than the implant material (e.g. steel or titanium) [22]. If the infecting bacteria are planktonic (single), then after adhering to the plasma protein-embedded bone tissue or implant, they will transform into a biofilm [6]. However, small aggregates of biofilm from the skin may also initiate the infection (Fig. 2A,C). A biofilm is defined as a cluster of bacterial cells embedded in an extracellular matrix, which is more tolerant towards antimicrobial agents and more capable of resisting the host immune defence mechanisms than planktonic bacteria [6,25–27]. Bacteria growing in a biofilm will persist, whereas planktonic bacteria will be susceptible to the antibiotics used to treat them (VIII) [6]. This increased antibiotic tolerance of biofilm bacteria is mainly due to their lower metabolic activity and their supporting extracellular matrix, which can bind and inactivate antimicrobial agents (Fig. 3B) [6]. Biofilm bacteria are 1000- to 10,000-fold more tolerant of antibiotics than their planktonic counterparts [28]. A bone infection biofilm will also mature over time, increasing its antimicrobial tolerance [22]. Because of this biofilm maturation, the probability of successfully treating a bone infection decreases dramatically from 80–90% to 30–60% if treatment is initiated more than 3–4 weeks after infection [22]. Osteomyelitis research has shown that eradicating tissue-based biofilms is extremely difficult. Antimicrobial therapy alone is often

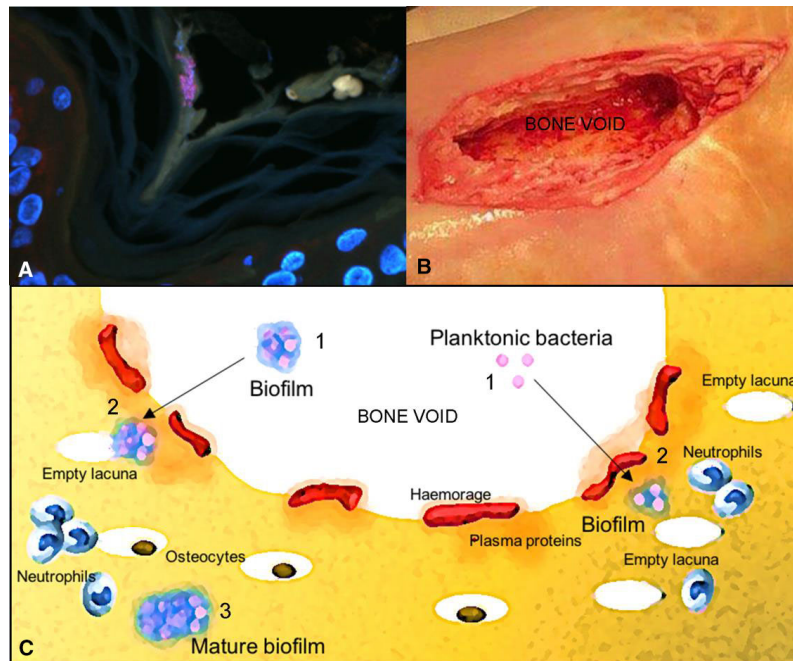


Fig. 2. Biofilm formation in bone tissue exposed during surgery. (A) Microscopy of human skin. Small aggregates of biofilm (pink) can be seen in a skin fold. (B) Bone exposed to debridement following an infection shows pinpoint bleeding of vital cortical bone tissue. (C) Biofilm aggregates from the skin (similar to those shown in A) can access the site of surgery (1); furthermore, single planktonic bacteria may also be introduced (1). The biofilm or planktonic bacteria may adhere to plasma proteins produced by any bleeding and also to dead bone tissue (indicated by empty lacunae), which promotes further biofilm formation (2). The mature biofilm (3) represents a potential remnant biofilm, that is not removed by the debridement and leading to recurrence of the infection.

unsuccessful in treating these infections, due to the high levels of antimicrobial tolerance acquired by mature biofilms, and implant removal and debridement of necrotic bone tissue may be necessary (Fig. 1) [16,29]. Even after removal of the infected implant and extensive debridement, prolonged systemic antibiotic treatment over several weeks may be needed to render the bone culture negative [16]. Moreover, the main reason for recurrence of IAO is bacterial biofilm survival in the bone tissue (Fig. 2C) [29].

CHAPTER 2

Animal models of bone infections

Non-rodent animal models of bone infections – Non-rodent animals such as sheep, goats, dogs, pigs and rabbits are being used more frequently in preclinical orthopaedic research due

to their relatively large bones, which are more accessible for the insertion of many orthopaedic devices than those of mice and rats [30]. This trend is also being reflected in the study of bone infections. Therefore, a comprehensive systematic review was carried out to provide an overview of previous studies on non-rodent (i.e. sheep, goats, dogs, pigs and rabbits) animal models of bone infections (IX). The aim was to identify differences in study design parameters, for example bacterial inoculation dose or infection time, among the five different animal species. The review also investigated the methodological quality of the studies and post-mortem recording and evaluation of pathology and microbiological factors. The review was based on a systematic search of two electronic databases (PubMed and Web of Science). This resulted in a total of 316 publications that fulfilled the inclusion criteria (i.e. experimental bacterial inoculation of animals

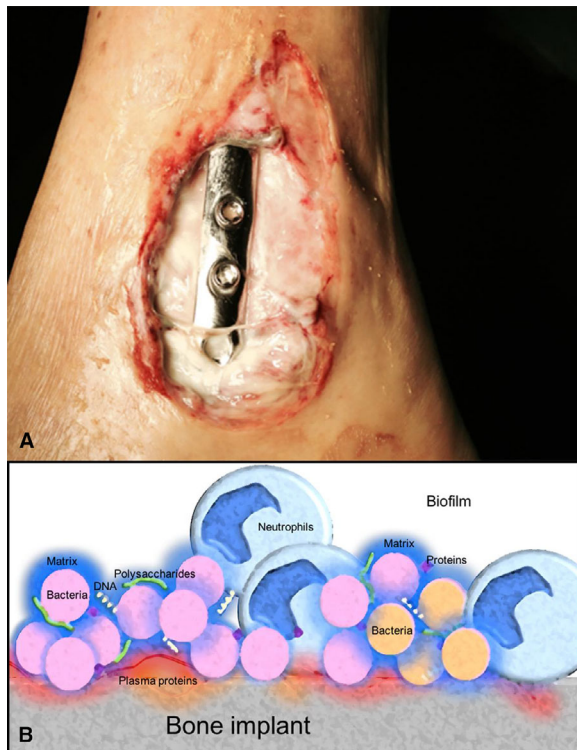


Fig. 3. Biofilm on bone implants. (A) Exposed osteosynthetic material on the ankle, surrounded by suppuration. A bacterial biofilm may grow on this foreign material, resulting in treatment failure. (B) Bacteria (shown in pink and orange) bind to plasma proteins covering the implant. These bacteria become embedded in the extracellular matrix (shown in blue), which comprises components derived from the host and bacteria. The matrix contains polysaccharides, DNA and proteins, and hamper antibiotic penetration. Some of the bacteria in the biofilm (shown in pink) grow normally, whereas others (shown in orange) grow more slowly; this also reduces the effect of some antibiotics. Host cells from the immune system will surround the biofilm, but the bacterial aggregates are too big to be ingested effectively by phagocytosis (IV).

in order to model any type of bacterial bone infection in humans; IX).

Findings related to study design: Since 2005, rabbits, pigs and sheep have been used more frequently as experimental animals to study bone infections that affect patients (Fig. 4; IX). While the use of ovine and porcine models is an alternative to previously preferred models developed in dogs, the increasing use of rabbit models reflects a demand for easy

handling, easy housing and low cost *in vivo* studies in a larger animal than a rodent [31]. Only a few differences were observed in the study design parameters among the five different animal species (e.g. sex, age, inoculation dose or time from inoculation to euthanasia; IX). However, porcine models, including the model described in this dissertation, were distinctive regarding a number of specific points. In particular, the mean bacterial inoculation dose was lower and the infection period (from inoculation to euthanasia) was shorter in pigs than in all other species (I–III, VII, VIII). Regardless of the animal species used or the type of bone infection modelled, the bacteria used most frequently for inoculation was *S. aureus*, although most of the studies did not report a specific identification code for the inoculated strain (IX). In general, studies on models that were based on traumatic inoculation directly into a specific bone reported using a significantly lower inoculation dose if an implant was inserted at the same time as the inoculum. Therefore, results from preclinical bone infection studies are consistent with those obtained in 1957 by Elek et al., who demonstrated that a foreign body can reduce the number of bacteria needed to establish an infection [32]. Elek et al. injected 7.5×10^6 colony forming units (CFU) of *S. aureus* into the skin of human volunteers, resulting in only 50% of the volunteers becoming infected and 100% of the cases being resolved. However, when Elek et al. inserted an implant and injected 100 CFU of *S. aureus*, all participants became infected and none of the infections were resolved.

Pathological remarks: The discriminative nature of animal models of bone infections can only be assessed by comprehensive pathological descriptions, that is aetiology, pathogenesis, development and characterization of bone lesions (Fig. 5). Therefore, it is necessary to perform appropriate pathological analyses, including macroscopic and histological descriptions and assessments of morphology, when using animal models of bone infections (IX). The major advantage of non-rodent bone infection models is the larger bone size, which facilitates a comprehensive pathological analysis of the infected bone. However, our

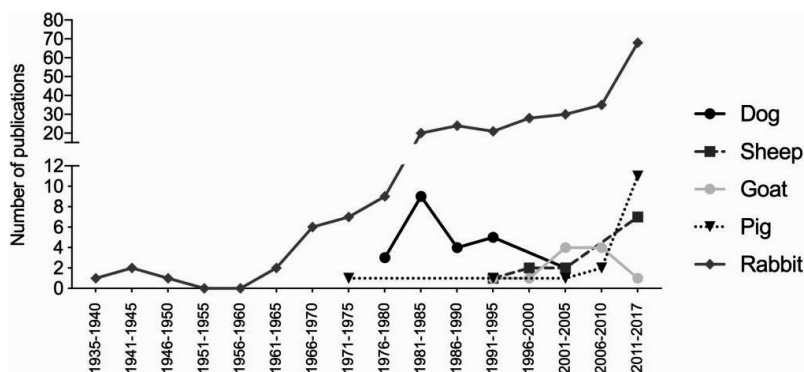


Fig. 4. Reports of non-rodent animal models of bone infections in humans (all types of bacterial bone infections) from 1935 to 2017. The number of publications reporting models developed in sheep, pigs and rabbits has increased, whereas models based on dogs have become less common. The broken line for rabbits is due to the interrupted y-axis (IX).

systematic review (IX) found that post-mortem macroscopic bone examinations were reported in fewer than 50% of the studies on dog, goat and rabbit models (IX). In general, histological results were reported more frequently (dog, 73%; sheep, 67%; goat, 36%; pig, 56%; and rabbit, 39%), although these histological findings were seldom scored semi-quantitatively (dog, 23%; sheep, 62%; goat, 50%; pig, 27%; and rabbit, 33%; IX). The preferred pathological macroscopic registrations for the animal species were 'sinus' and 'purulent' drainage, which are confirmatory diagnostic criteria for bone infections in humans [16,33]. In contrast, the registration of histological parameters varied significantly among the five different animal species (IX).

Microbiological remarks: Our review demonstrated that post-mortem microbiological examinations of bone tissue and implants were performed in approximately 80% of the studies, regardless of the animal species (IX). However, a quantitative assessment of the bacterial load was only reported in approximately 50% of the times. Many of the models were used to examine different antimicrobial interventions, and the lack of quantitative microbiology makes it difficult to reproduce reported effects objectively. Our review also found that only 30% of the studies investigating an antimicrobial intervention reported complete sterility; that is, all animals given the highest dose showed sterility of tissue and/or implants post-

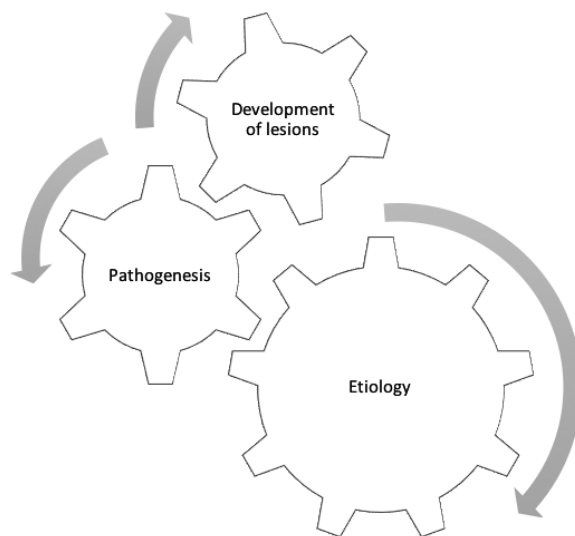


Fig. 5. Disclosure of discriminative value in animal models of infectious diseases. All animal models of bacterial infections are generated in the same way: an aetiology is introduced and lesions develop via a specific pathogenesis. To evaluate the different animal models of bone infections in terms of their capacity to reproduce the disease of interest, bone pathology must be assessed (i.e. aetiology, pathogenesis and development and appearance of lesions) using comprehensive macroscopic and microscopic examinations.

mortem (IX). This failure to report sterile outcomes means that valuable information regarding osseous-effective antibiotic doses for *in vivo* use has been lost. In many studies, a significant reduction in bacterial load was

reported post-mortem (IX), but what is the difference between a 1000-fold reduction from 10^7 CFU (inoculation dose) and a 100-fold reduction from 10^4 CFU in terms of clinical significance? [34] A study design should always aim to completely eradicate infection. An intervention which almost eliminates the bacterial load may have an impact, but a re-established biofilm infection is likely. A recent review of animal models of bone infection by Moriarty et al. suggested that the clinically relevant efficacy of anti-infective interventions should be assessed in terms of the complete eradication of infection [34].

Methodological quality: In general, the methodological quality of studies on non-rodent animal models of bone infections was low because randomization, power calculations and blinding were seldom reported (IX). However, previous research has shown that the absence of blinding can lead to the effect size of an intervention being overestimated [35,36]. Therefore, blinded quantification of pathological and microbiological findings may improve the applicability of test results obtained from animal models of bone infections (IX). Furthermore, we found that study design data (e.g. age, sex, bacterial strain and inoculation dose) were often omitted, making it difficult to compare and reproduce findings among studies (IX). Our review of non-rodent models supports some of the criticisms regarding methodological quality and lack of assessments that were raised recently by Moriarty et al. [34] The degree of overlap between these two reviews highlights the current need for improvements in preclinical bone infection studies (IX) [34].

Standard study template guidelines: In conclusion, poor reporting of study design and low methodological quality were common problems in many studies on non-rodent animal models of bone infections (IX). Furthermore, histopathological, standard registration and infection quantification procedures varied significantly among these studies. Consequently, we generated guidelines for standard reporting of animal models of bone infections (Table 1; IX). These guidelines are designed to improve the reproducibility of findings among studies based on similar models and models in

different species. Thus, the guidelines may be used to help authors to write clear, accurate, concise manuscripts that describe bone infection models (IX).

Modelling of bone infections in pigs – The ideal animal species for modelling of human bone infections should have molecular, cellular and structural features that are similar to those of patients, a well-characterized immunological profile, and large robust bones to ensure that medical and surgical interventions applied in the model will reflect clinical practice [31]. However, these features vary significantly among different animal species. Because our systematic review of non-rodent bone infection models (IX) identified very few differences among study design parameters, the selection of an appropriate animal species is extremely important. Therefore, the next section focuses on the advantages of using pigs to model human bacterial bone infections. Previously, pigs were primarily used as experimental animals to study toxicology, metabolism, cancer and xenotransplantation [37]. However, during the last 10 years there has been an increase in the number of porcine models used to study bacterial infections in patients, primarily focusing on systemic, gastrointestinal, respiratory, heart and bone infections [37].

The pig as an experimental animal: Pigs are often used as experimental animals because some of their key characteristics are similar to those of humans, including their size, anatomy and physiology [38,39]. The complete genome of the domesticated pig has been sequenced, and many laboratory reagents specific for porcine tissue have become available [38,40]. Porcine models of human bacterial infections have mainly been developed in conventional pigs raised for slaughter or, less frequently, in minipigs [37]. The major difference between farm pigs and minipigs is growth rate. The grow rate of a conventional pig is rapid (1 kg at birth, 100 kg at 4 months and adult body weight >200 kg) compared to that of a minipig (0.5 kg at birth, 12–14 kg at 4 months and adult body weight of 40–80 kg) [37]. Therefore, minipigs are more favourable for modelling of adult patients. However, the majority of pigs used to model adult human bacterial

Table 1. Overall principles that are of crucial importance when bone infection models are developed, validated and reported (IX)

Guideline for standard reporting of animal models of bone infections	
General aspects	Type of bone infection modelled; Definition of infection in the model
Animal	Species, age, sex, breed, producer
Pathogen	Bacterial strain, including identification number, inoculation dose, and volume
Implant or prosthesis	Type, material, size, producer
Pathogen (+implant) into the animal: inoculation procedure	Haematogenous inoculation route <ul style="list-style-type: none"> • Vessel • Bone trauma prior to inoculation • Insertion of bone implant prior to inoculation Traumatic inoculation route (directly into a bone) <ul style="list-style-type: none"> • Description of bone surgery • Description of insertion of implants • Description of inoculation procedure
Pathogen (+implant) within the animal: infected animal	Monitoring development of bone infection; Monitoring systemic disease; Disease management (<i>e.g.</i> analgesic treatment); Time frame (from inoculation to euthanasia)
Post-mortem evaluation of infection	Local pathology of the inoculated bone, including quantification Local microbiology of the inoculated bone and implant, including quantification Systemic pathology and microbiology (<i>e.g.</i> embolic spread of local infection)
Intervention	Aim Time of intervention in relation to inoculation Description of intervention
Methodological quality	Randomization of animals into study groups Blinding when quantifying pathology and microbiology Power analysis

infections, including bone infections, were reportedly less than 12 weeks old [37]. More than one-third of all studies describing porcine models of infectious diseases in humans have been based on specific pathogen-free (SPF) pigs [37]. SPF is a term used in swine management to describe animals that are guaranteed free of particular infectious diseases, although they may have been exposed to many different pathogens [41].

Osteological advantages: Pigs are considered comparable to humans with respect to bone anatomy and morphology. One study of the microstructure of a porcine femur reported that the basic structure of compact bone consisted primarily of vascular plexiform bone with dense haversian systems in the middle

[42]. The quantity of osteonal bone increases with age and the structure of porcine bone is more similar to that of human bone than is the structure of bones from other species such as sheep or goats [43–45]. The cancellous bone structure of pigs is similar to that of humans, although the trabecular network of porcine bone is denser [46]. In addition, the density and mineral composition of porcine and human bones are similar [43,45,46]. Aerssens et al. compared femoral cortical and lumbar trabecular bone samples from dogs, pigs, chickens and rats with those from humans and found that the mineral content of canine and porcine femora was similar to that of the human femur, whereas the mineral content of rat bones was the most dissimilar [47]. Furthermore, bone remodelling and cortical bone

mineralization rates in pigs and humans are similar [43,44,46]. Finally, a recent study on the porcine IAO model inoculated with saline demonstrated that the local expression pattern of inflammatory and bone regulatory genes in bone tissue exposed to surgery was similar to that reported in human studies [10].

Immunological advantages: The porcine immune response to bacterial infection is also very similar to that of humans; that is, many key proteins of the human and porcine immune systems are structurally and functionally similar [38,48]. The animals most frequently used to investigate the immune response to bacterial infections in patients, including bone infections, are mice [49,50]. However, recent research has demonstrated that several aspects of the immune response to bacterial infections differ substantially between mice and humans [38,49,51]. For example, the human inflammatory genes interleukin (IL)-26, chemokine ligand type 8 (CXCL8) and chemokine receptor type 1 (CXCR1) have no homologues in mice and neutrophils are the predominant leucocytes in human peripheral blood, whereas lymphocytes are predominant in mice [38,52,53]. Pigs can also express IL-26, CXCL8 and CXCR1 in response to bacterial infections and neutrophils are the predominant blood leucocytes [38]. A recent review reported that all *in vivo* studies of cytokine expression in IAO and PJI have been carried out in mice or rats, so apart from studies using human samples, all current data regarding cytokine production and the molecular pathways involved in bone infections depend on rodent models [54]. However, the porcine IAO model has now been used to study the expression of inflammatory cytokines and mediators within 5, 10 and 15 days of bone infection [11]. More precisely, expression analysis of infected bone tissue revealed local upregulation of several positive acute phase proteins (APPs) such as serum amyloid A3 (SAA3) and complement component 3 (C3) [11]. This is the first description of local osseous APP regulation in response to bacterial bone infection. However, only small changes in APP expression were observed in the liver, and serum APP levels decreased over time [11]. Thus, the osseous

upregulation of APPs in CO appears to be part of a local response [11].

All the text books on bone pathophysiology describe how bone loss due to infectious osteomyelitis is caused by an inflammatory response that increases osteoblastic RANKL expression [55]. Binding of RANKL to the RANK receptor on osteoclastic precursors and mature osteoclasts induces both osteoclastogenesis and osteoclastic bone resorption [55]. The connection between increased RANKL expression and infectious bone loss was established by *in vivo* studies using murine bone infection models and *in vitro* studies investigating murine osteoblastic cell lines grown together with *S. aureus* [56–58]. However, it has not been possible to confirm the murine-based results using biopsies from patients with CO [59,60]. Surprisingly, in the porcine IAO model, the expression of RANKL [with references to text books and scientific literature] was reduced in 5-, 10- and 15-day-old osteolytic bone infections [13]. This demonstrates that the classic RANK/RANKL pathway probably not is upregulated in humans or pigs with bone infections. Thus, the value of murine models for investigating infectious bone pathophysiology is questionable. A significant upregulation of IL-26 was observed in the porcine IAO model and IL-26 reportedly inhibits RANKL-induced osteoclastogenesis. As described previously, IL-26 has no homologue in mice. The gene expression results suggest that enzymatic bone destruction may occur as an alternative to RANKL-induced bone loss because significant levels of, for example, matrix metalloproteinase 1 (MMP1) expression were observed [13,60,61].

In the future, *in vitro* immune biology observations considered relevant for human bone infections must be reproduced in reliable animal models. This is important because new treatments for bone infections will include not only antimicrobial therapy but also modulation of the pathophysiology (e.g. stimulation of bone formation or inhibition of bone loss). Based on the results from the gene expression studies in the porcine IAO model, IHC procedures are being developed to target SAA, C3, IL-26 and MMP1, and these procedures are being tested on biopsy samples from patients

with CO. Hopefully, these studies will reveal new diagnostic and prognostic biomarkers.

Spontaneous infections: As in humans, bone infections also occur spontaneously in pigs. In Denmark, more than 100,000 pigs are annually diagnosed at slaughter with purulent lesions within their bones [62]. Lesions are most frequently haematogenous, and a common portal of entry is tail lesions due to tail biting [63,64]. These bone lesions are located in the metaphyseal area of long bones, vertebra and in the costochondral junctions of the ribs (Fig. 6) [63,64]. Common aetiologies of osteomyelitis in pigs include *S. aureus* and *Trueperella pyogenes* [63,64]. Haematogenous osteomyelitis is also observed infrequently in other species used for modelling of human bone infections such as small ruminants, pet dogs and rabbits [65]. However, the most common aetiology in rabbits, where the lesion is often within the jaw, is *Pseudomonas aeruginosa* [66]. There are no data regarding spontaneous naturally occurring bone infections in rodents. Recently, spontaneous infection disease models have been embraced because they demonstrate robust superiority over experimental models [67]. Naturally occurring bacterial osteomyelitis in slaughter pigs displays patho-morphological similarities to bone infections in patients (IV). Furthermore, recent research has identified several inflammatory biomarkers that were expressed in both the porcine IAO model and in lesions from slaughter pigs with spontaneous osteomyelitis [11]. In addition, the



Fig. 6. Chronic osteomyelitis with secondary arthritis in the front leg of a Danish slaughter pig.

biomarker expression pattern in both experimental and naturally infected pigs was similar to that observed in biopsy samples from humans with CO [11]. Thus, slaughter pigs with CO represent an untapped source that may be used to investigate the host immune response to human bone infections.

CHAPTER 3

A porcine model of implant-associated osteomyelitis (IAO)

Animals and inoculum – A novel porcine model of IAO was developed (II, III) and applied in different experimental studies (I, V–VIII). The model was based on female pigs (Danish Landrace) obtained from SPF herds. The animals were group-housed and were allowed to acclimatize for 7 days before the surgical procedures. Pigs weighing 30–40 kg were used to develop the model, whereas pigs weighing 80–90 kg were used in the antimicrobial pharmacokinetic studies (I, VII). The porcine IAO model replicated exogenous pathogenesis associated with IAO in humans [16] and was therefore based on direct inoculation of *S. aureus* bacteria into the right tibia during a minor surgical procedure. The *S. aureus* strain used was S45F9, originally isolated from an embolic porcine lung abscess [68]. This strain was chosen because it had previously been effective in inducing various bacterial infections in pigs, including haematogenous osteomyelitis, and showed higher virulence in pigs than two other human *S. aureus* strains (NCTC8325-4 and UAMS1) in previous studies on haematogenous osteomyelitis and endocarditis [69,70]. Pathogenic bacterial strains may have evolved separately with different immune defences found in different species [71]. Therefore, human pathogens do not necessarily cause predictable infections in animals [72]. A well-characterized inoculum is essential for obtaining reproducible results in animal models of human infectious diseases. Therefore, the whole genome of S45F9 was sequenced, and the strain identified as belonging to *S. aureus* Protein A *spa*-type t1333 and multilocus sequence type (MLST) ST433 [73]. The strain has genes encoding several toxins, including phage-associated enterotoxin, exotoxins and

superantigen [73]. Biofilm production by *S. aureus* S54F9 was evaluated using a crystal violet *in vitro* microtiter biofilm assay and compared to that of biofilm-producing strain RN4220 (VI). The production of biofilm was identical for the two strains (VI). An inoculum of 10^4 CFU of S45F9 in 10 μ L sterile saline was the minimum 100% effective dose for inducing IAO in the porcine model (III).

Surgical inoculation procedure and perioperative period – Anaesthetized pigs were placed in right lateral recumbency exposing the medial side of the right tibia. The porcine IAO model was based on an implant cavity of 4 mm \times 20 mm drilled using a K-wire and

located parallel and distal (10 mm) to the proximal tibial growth plate (II, III). Anatomical guidelines were created to standardize the point of drilling into the tibia (Fig. 7). These guidelines ensured that the location of the implant cavity was precisely defined.

The inoculum, or sterile saline for control animals, was injected into the implant cavity and then a small steel implant (2 \times 15 mm) was inserted (Fig. 8; II, III, V–VIII). Once the implant was inserted, the periosteum, subcutaneous tissue and skin were sutured (Fig. 8; II, III, V–VIII).

Following bone surgery, the pigs were inspected several times each day throughout the study period. All animals were provided

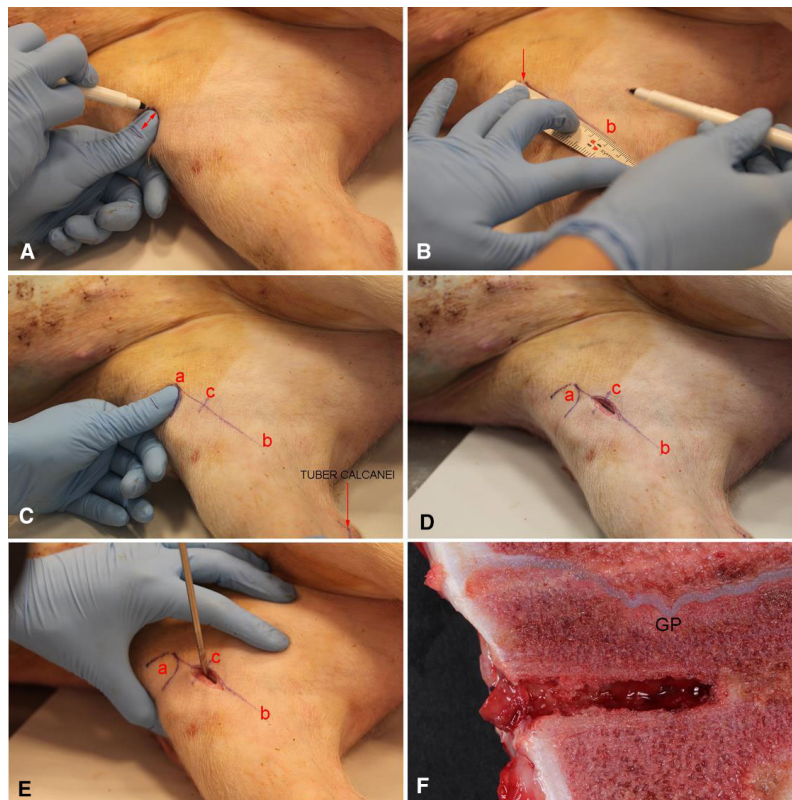


Fig. 7. Position of the drill cavity in the porcine IAO model. The pig is positioned in right lateral recumbency. (A) A distance of 1.5 cm is measured on the investigator's thumb and marked with a pen (arrow). The thumb is placed over the knee joint with the mark beginning at the cranial border of the knee and a line is drawn around it. (B) A line is drawn (b) from the top of the arch (arrow) towards the tuber calcanei. (C) A total of 2 cm is measured from the top of the arch (a) along line b. At this point, a short perpendicular line is drawn (c). (D) An incision is made through the skin, subcutaneous tissue and periosteum along line b, at the level of line c. (E) A 2-cm hole is then drilled where lines b and c cross. The drill should be perpendicular to the bone and angled slightly distally to the growth plate. (F) The result is a drill cavity located parallel to the growth plate (GP) in the metaphyseal area of the proximal tibia.



Fig. 8. Inoculation procedure in a porcine model of IAO. (A) Equipment used for inoculation. (B) An incision is made through the skin, subcutaneous tissue and periosteum of the proximal tibia (see Fig. 7). (C) The periosteum is loosened a few mm along the incision line. (D) A 4-mm K-wire is drilled 20 mm into the trabecular bone tissue. E: Following haemostasis of the drill cavity, the inoculum (*Staphylococcus aureus*) is injected. (F) Next, a steel implant (2 × 15 mm) is inserted. (G) The periosteum is closed over the implant. H: Finally, the soft tissue and skin are closed.

with daily oral non-steroidal anti-inflammatory drugs (NSAIDs) for analgesia, whether they had been inoculated with bacteria or saline (III). Some pigs were lame after recovery from anaesthesia; however, these pigs could still use the inoculated leg and walk freely around the pen (II, III). A few pigs developed persistent lameness with no weight bearing at all, and intramuscular opioid injections were administered until these pigs were euthanized. Impaired ability to stand, anorexia and systemic signs of

sepsis, for example depressed respiration and fever, were set as human endpoints.

Time frame: Optimally, animal models of bone infections should have a time frame (time from inoculation to euthanasia), which reflects the disease stage of interest, for example acute or chronic [34]. However, developing animal models of chronic infectious diseases is problematic due to ethical issues related to housing animals with experimentally induced chronic

infections, for example the long periods of suffering associated with the development of chronic symptoms. Furthermore, it may be difficult to maintain an infection induced in healthy animals, which may otherwise resolve spontaneously [72]. In the first study of the new porcine IAO model, animals were euthanized 2, 4 or 6 days after inoculation (II). Due to the high virulence of the porcine *S. aureus* strain [73], bone lesions comparable to those observed in human osteomyelitis developed, and pus, sequestra and granulation tissue were all observed [16,17] (II). Therefore, a time frame of 5 days was used in subsequent studies (I, III, V–VIII).

Post-mortem quantification of bone infection – The porcine IAO model successfully replicated pathogenesis associated with bacterial infections during bone surgery, that is by the insertion of contaminated implants or prostheses in patients. We developed an objective protocol to quantify lesions and infections so that the model could be used in intervention studies to identify infections and differences between study groups (I, II, III, V–VIII). This quantification protocol was based on computed tomography (CT) scanning, pathological examinations and microbiological analyses.

CT-scanning: After the pigs were euthanized and the bone implants were removed, each right hind leg was CT scanned (slide thickness = 2 mm) and reconstructed using a soft tissue algorithm (III). OsiriX Lite software (ver. 10.0.3; Pixmeo, Geneva, Switzerland) and CT volumetry were used to calculate the 3-dimensional volume of each implant cavity plus surrounding bone lesions [74]. In all animals inoculated with saline, the estimated volume included only the implant cavity (Fig. 9), whereas inoculation with bacteria resulted in osteolysis around the implant cavity and significantly increased volumes (Table 2, Fig. 9; III, VIII). In some of the infected pigs, both trabecular and cortical bone sequestra were present.

Macroscopic pathology: Pigs inoculated with saline showed slight subcutaneous, non-purulent inflammation at the surgical sites (Fig. 10A,B; II, III, VIII). Furthermore, the

periosteal sutures in all control animals remained intact (Fig. 10A,B; II, III, VIII). However, in infected animals, swelling was observed around the surgical sites (Fig. 11A,B; I–III, VII, VIII), and when the sutures were opened and the subcutis was peeled back, purulent soft tissue inflammation connected to the bone implant cavities was observed (Fig. 11C; I–III, VII, VIII). The right tibia was sectioned sagittally, through the implant cavity. The implant cavities of animals inoculated with saline had a regular outline with no signs of infection (Fig. 10C,D; II, III, VIII). In contrast, macroscopic signs of osteomyelitis (e.g. pus and pale dead bone tissue) were observed around the implant cavities of animals inoculated with bacteria (Fig. 11D,E; I–III, VII, VIII). Additionally, infected animals had enlarged implant cavities with irregular outlines (Fig. 11E).

Histopathology: Pathological changes around the implant cavity were described as occurring within the peri-implant pathological bone area (PIBA; Fig. 12; I–III, V–VIII). The PIBA size was estimated based on the largest observed distance extending from the edge of the implant cavity to normal bone tissue (Fig. 12). In saline-inoculated animals, the surgical inoculation procedure *per se* resulted in thermal bone necrosis and debris around the implant cavity (Fig. 12B; II, III) [10]. In addition, a small amount of inflammatory cellular infiltration occurred. These changes resulted in PIBA of less than 1.5 mm for saline-inoculated animals (II, III). This finding is consistent with previous studies, which showed that changes in bone structure (primarily osteonecrosis) occurred up to 1.2 mm from inserted K-wires [75]. A very different PIBA pattern was observed in animals infected with bacteria (Fig. 12A; I–III, V–VIII). In these animals, a layer of cells that included fibroblasts, neutrophils (sometimes arranged as micro-abscesses), macrophages, giant cells and bone debris was observed around the implant cavity (Fig. 12A). This layer was surrounded by osteonecrotic trabecular bone intermixed with the same cell types and active osteoclasts observed in resorptive lacunae of the necrotic bone trabecula (Fig. 13A). At the periphery of PIBA, osteoblast and fibroblast proliferation

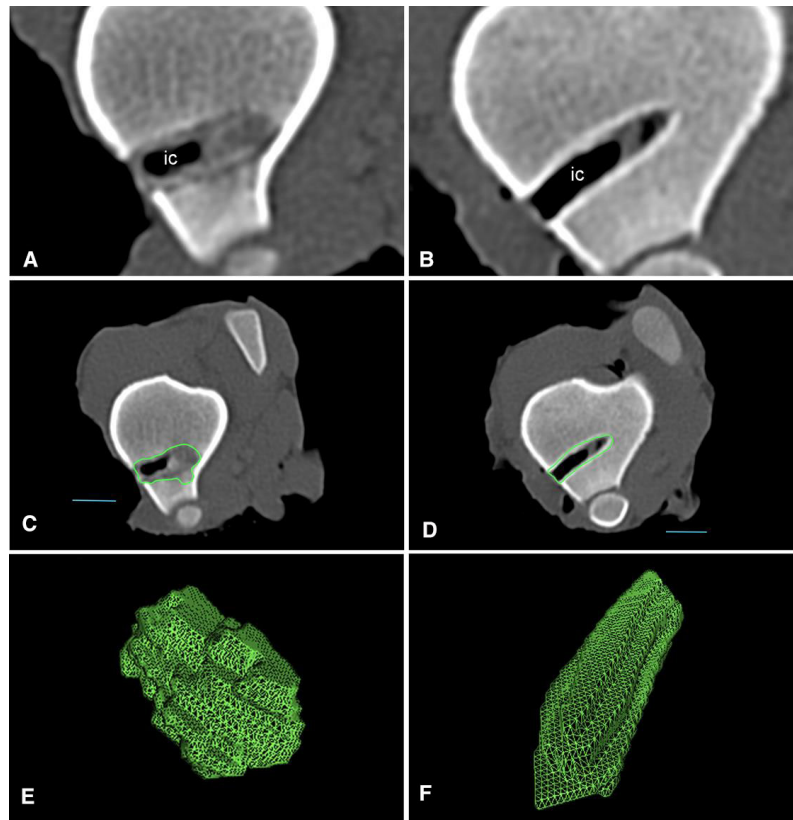


Fig. 9. Computed tomography (CT) scans of a porcine model of IAO inoculated with *S. aureus* (left panel: A, C, E) or saline (right panel: B, D, F). (A) The implant cavity (ic) is enlarged and the outline is irregular. (B) In contrast, the implant cavity (ic) of control animals is regular and sclerotic. (C and D) The outlines of the implant cavity and surrounding bone lesions, if present, were defined as regions of interests (ROIs: green line) on each image using a series of consecutive 1-mm scans. The blue line is 10 mm long. (E and F) The total volume of the implant cavity plus the lesion was estimated using the defined ROIs.

and the associated production of osteoid and collagen were observed (Fig. 13B). All of these pathological changes resulted in a mean PIBA of 3 mm in the porcine IAO model (I–III, V–VIII). As described in Chapter 1, suppurative inflammation can lead to osteoclast activation, secretion of proteolytic enzymes from inflammatory cells and activation of matrix metalloproteinases, which together result in the breakdown and collapse of bone matrix [20]. This explains why osteolysis occurs in the PIBAs of infected animals, together with implant cavity enlargement and the irregularity of cavity contours (I–III, V–VIII).

An evaluation of NG infiltration is included in the diagnostic guidelines for several types of human bone infections. [16,33,76,77] Therefore, this was also included in the histological evaluation of the porcine IAO model (II, III,

V, VIII). The number of NGs inside each PIBA was estimated using the method developed by Morawietz et al. (III) [78]. First, potential hot spots rich in NGs were identified at low magnification. These areas were then evaluated at high magnification (400 \times), and all clearly identifiable NGs were counted. In each HPF, a maximum of 10 NGs were counted. Ten HPFs were examined in this way, resulting in a maximum count per pig of 100 NGs [78]. The threshold for a histopathological differentiation between infected and sham (saline) inoculated animals was 40 NGs in 10 HPFs (sensitivity = 92%, specificity = 90%; III). In the first study of the porcine IAO model (II) and the study of histological changes associated with reduced antimicrobial penetration into infected bone tissue (V), the histological criteria developed

Table 2. A porcine model of IAO. The table provides details of the host, pathogen and the infection, based on clinical definitions and classification systems

Overview of a novel porcine model of implant-associated osteomyelitis (I–IX)	
Animal	Pigs, Landrace (SPF), female, 35 kg BW
Pathogen	<i>S. aureus</i> (S54F9)
Bone	Tibia
Implant	2 × 15 mm steel
Inoculation dose with 100% success rate	10 ⁴ CFU in 10 µL
Embolic spread from infected bone	No
Pathogenesis [16]	Exogenous
Time frame	5 days
Classification IAO [2,16]	Early
Inflammation stage [20]	Subacute
Peri-prosthetic membrane oft type [88]	II
Clinic infection stage [16]	Acute
Cierny-Mader stage [18]	3A
Fulfilling the definitions of IAO in humans: [16]	
Pus surrounding the implant	Yes
Sinus tract communicating with the implant	Yes
Identical microorganism in at least two samples (biopsies, exudate, sonication fluid)	Yes
Presence of > 5 neutrophil granulocytes per 10 high-power fields in a biopsy	Yes
Quantification of inflammation and infection	
PIBA size (mean ± SD)	3 ± 1,29 mm
Neutrophil count (mean ± SD)	85 ± 26
3D volume of implant cavity + surrounding lesion(mean ± SD)	0.9 ± 0.6 cm [3]
CFU on implants (mean ± SD) in mL sonication fluid	10 ⁶ ± 10 ⁴ CFU

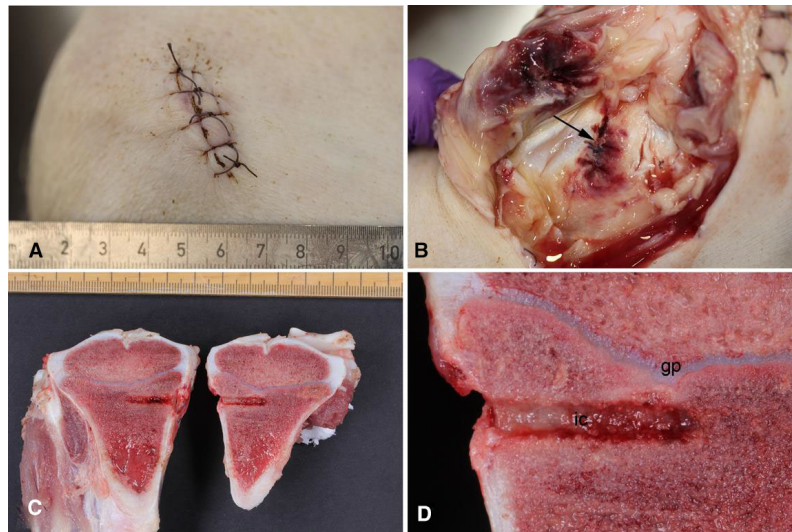


Fig. 10. Macroscopic pathology in a porcine model of IAO inoculated with saline. (A) The operation wound sutures are intact and no exudate is visible. (B) Opening of the wound shows some inflammation is present with hyperaemia in the subcutaneous tissue. The sutures in the periosteum are intact. (C) The implant has been removed and sagittal sectioning of the bone exposes the implant cavity. (D) Close-up of the implant cavity (ic) distal to the growth plate (gp). No signs of bone inflammation are present.

by Pandey et al. [79] and Feldman et al. [80] were used, respectively, to determine whether an infection was established. These criteria are

more similar to the newly developed diagnostic criteria for fracture-related bone infections [77]. However, the scoring system developed

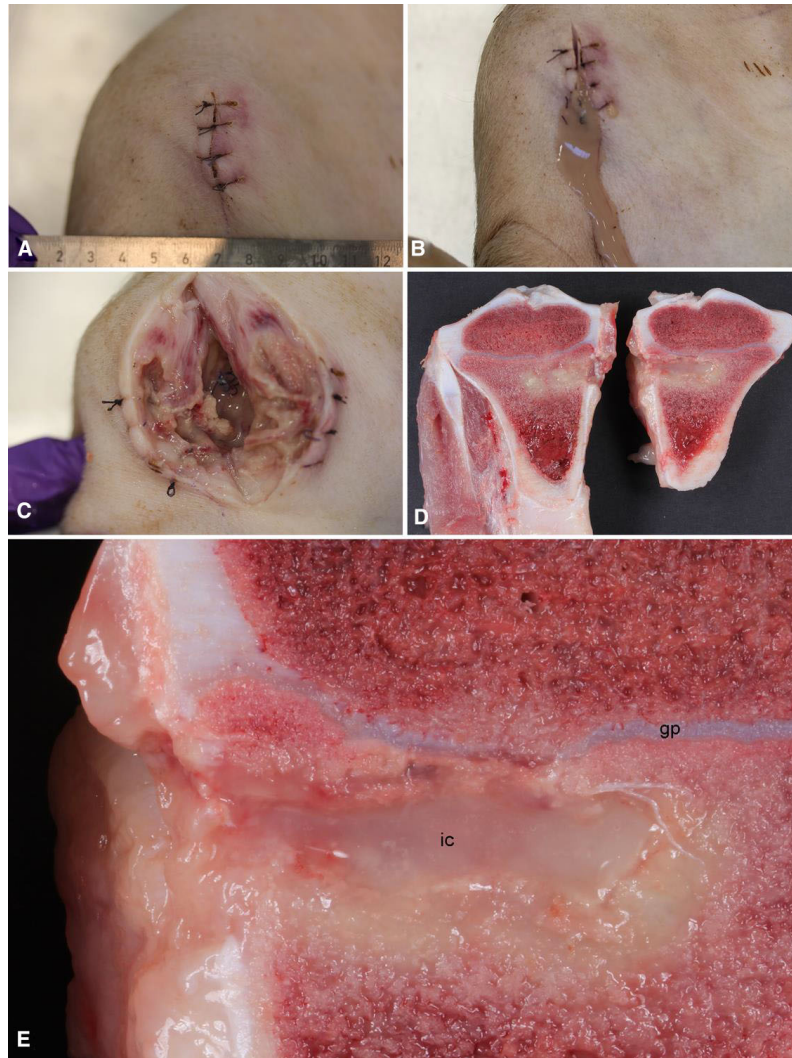


Fig. 11. Macroscopic pathology in a porcine model of IAIO inoculated with *Staphylococcus aureus*. (A) The operation wound sutures are intact, but the wound is swollen and hyperaemic. (B) Opening of the wound results in leakage of pus. (C) Completely opening the wound down to the periosteum shows purulent soft tissue inflammation connected to the bone implant cavity. The periosteum sutures are not completely intact. (D) The implant has been removed and sagittal sectioning of the bone exposes the implant cavity. (E) Close-up of the implant cavity (ic) distal to the growth plate (gp). The implant cavity is filled with pus and the surrounding bone tissue shows necrotic and purulent inflammation.

by Morawietz et al. was better for distinguishing among interventions because this estimated the number of infiltrated NGs [78]. Finally, we recorded whether bacteria were present within the PIBA and, in selected cases, IHC staining for *S. aureus* was performed (Fig. 14; II, III, V, VI, VIII). The sizes (diameter) of bacterial aggregates within bone tissue from patients with different types of bone infections were recently estimated as ranging from 5–50 μM

[7]. In general, the maximal biofilm size has been estimated as 200 μM [7]. In the porcine model, all *S. aureus* aggregates within PIBAs were less than 84 μM ; therefore, these are comparable with those observed in patients (III). Massive accumulation of neutrophils and macrophages occurred around bacterial aggregates localized within PIBAs (I–III, V–VIII). However, bacterial clearance was significantly impaired, indicating deficient granulocyte

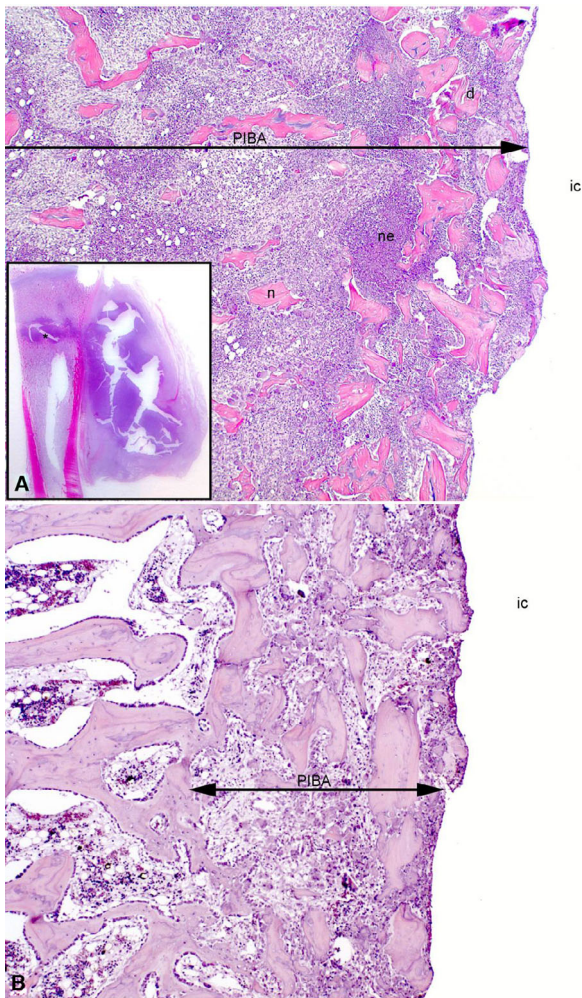


Fig. 12. Histopathology in a porcine model of IAO inoculated in the right tibia with *Staphylococcus aureus* (A) or saline (B). (A) The insert shows the entire bone lesion and the associated soft tissue abscess. The asterisk (*) indicates the location magnified in the large image. The peri-implant pathological bone area (PIBA) was defined as the perpendicular distance between the implant cavity (ic) and the appearance of normal bone architecture. Bone debris (d) created by drilling the implant cavity was located nearby. Neutrophil (ne) accumulation, necrotic bone tissue (n) and osteoclast proliferation occur within the PIBA. Haematoxylin and eosin (HE). (B) Here, the PIBA was significantly smaller compared to the PIBA created by bacterial inoculation. HE. (VIII).

function or bacterial resistance to phagocytosis [81]. Previous research has shown that the interaction of macrophages and neutrophils with a non-phagocytosable surface, such as an

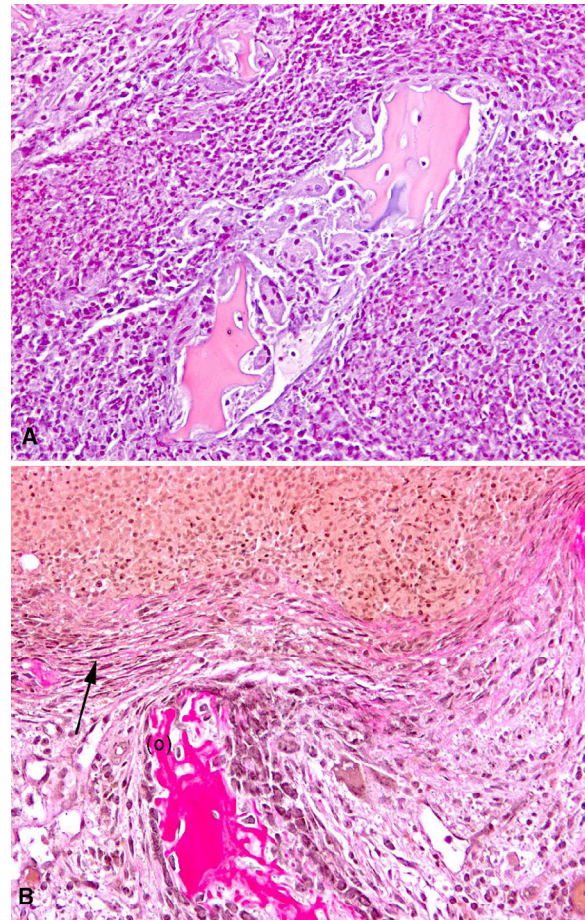


Fig. 13. Histopathology in a porcine model of IAO inoculated in the right tibia with *Staphylococcus aureus*. (A) Close-up of a necrotic bone trabeculum surrounded by bone resorbing osteoclasts. HE. (B) Fibroblast proliferation (arrow) and pink osteoid (o) production by active cubic osteoblasts were observed at the edges of the PIBA. Van Gieson.

orthopaedic implant or a large biofilm, impairs phagocytosis [81]. Therefore, the IAO model also elucidates the clinical paradox of microbial persistence despite the presence of numerous granulocytes around an orthopaedic implant [81].

Microbiology: Following euthanasia, swabs were taken from the soft tissue associated with the surgical sites and from the implant cavities of all animals. Inoculation with 10^4 CFU resulted in positive cultures of *S. aureus* with the same *spa*-type as that used for the inoculations (I–III, VII, VIII). Only rarely was

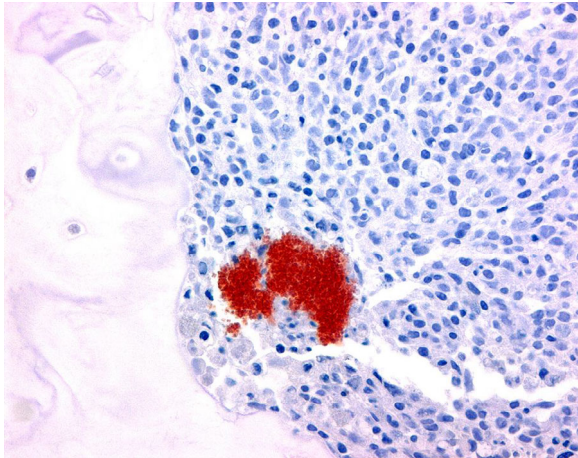


Fig. 14. Immunohistochemical (IHC) staining of a porcine model of IA0 inoculated in the right tibia with *Staphylococcus aureus*. Red coccoid *S. aureus* bacteria surrounded by inflammatory cells near trabecular bone. IHC staining with a primary antibody against *S. aureus* (IV).

contamination with porcine streptococci or non-pathogenic porcine *S. aureus* strains of another *spa*-type present in both control and infected animals (II). Cultivation based on cotton swabs is not recommended for making microbiological bone infection diagnoses in patients [82]. However, in the porcine model, this method reliably confirmed the presence of infections and the results could be correlated with those from other tests, for example histology and sonication of implants. Recent research showed that sonication (i.e. implants are sonicated in an ultrasonic bath and the resulting fluid is cultured) improves the detection of microorganisms attached to an implant [83]. Therefore, sonication was used to estimate the number of bacteria attached to implants in the porcine model and the mean number of attached bacteria was approximately 10^6 CFU/mL sonication fluid (IX).

Embollic spread from the local bone infection – Following euthanasia, necropsies were performed (I–III, VII, VIII). The pigs were placed in dorsal recumbency, the abdomen and thorax were cut open across the midline, and all organs were inspected and palpated *in situ*. Tissue samples were taken from the lungs, liver, right kidney and spleen, and these were used for histological examinations. However,

no macroscopic or histological lesions indicating embolic spread of the inoculum were observed in any animals (I–III, VII, VIII). In addition, a lung sample was taken for microbiological examination because porcine lungs trap blood-borne pathogens due to the presence of specialized pulmonary intravascular macrophages [84]. All samples were sterile, indicating no haematogenous bacterial spread in any of the animals.

Comparison with previous porcine bone infection models – Previously, pigs have only been used three times for modelling traumatic bone infections using bacterial inoculation directly into a specific bone: in 1975, 1993 and 2001 [85–87]. The first model, developed by Koschmieder et al., established bone infection by intramedullary inoculation of *S. aureus* (2×10^8 CFU) into a femoral cortical window [85]. This model was used to test the effects of a gentamicin-impregnated bone cement over a 16-day infection period. The second model was developed in minipigs by Patterson et al. [86]. In this model, three strains of *S. aureus* (10^9 CFU) and a bone sclerosing agent, which was used to induce bone necrosis, were introduced into the right mandible by intramedullary inoculation [86]. The infection time in this model was 12 weeks. The final model was established by inoculating 2×10^3 CFU of *S. aureus* into a diaphysis fracture line using an 18 G needle [87]. The animals were euthanized after 28 days, and the cellular immune response was evaluated [87]. Consequently, the present porcine IA0 model involves a significant reduction in the number of injected bacteria, compared to the former models. Furthermore, only the present porcine IA0 model (inoculated with 10^4 CFU) and the model developed by Patterson et al. reported a 100% success rate; that is, all inoculated animals developed an infection that was positively identified by microbiological tests (I, III, VII, VIII).

Comparison with IA0 in humans – Our novel porcine IA0 model replicates exogenous pathogenesis via surgical contamination with a highly virulent *S. aureus* strain (Table 2) [16]. The time frame of 5 days resulted in subacute suppurative bone inflammation (I–III, V–VIII). The

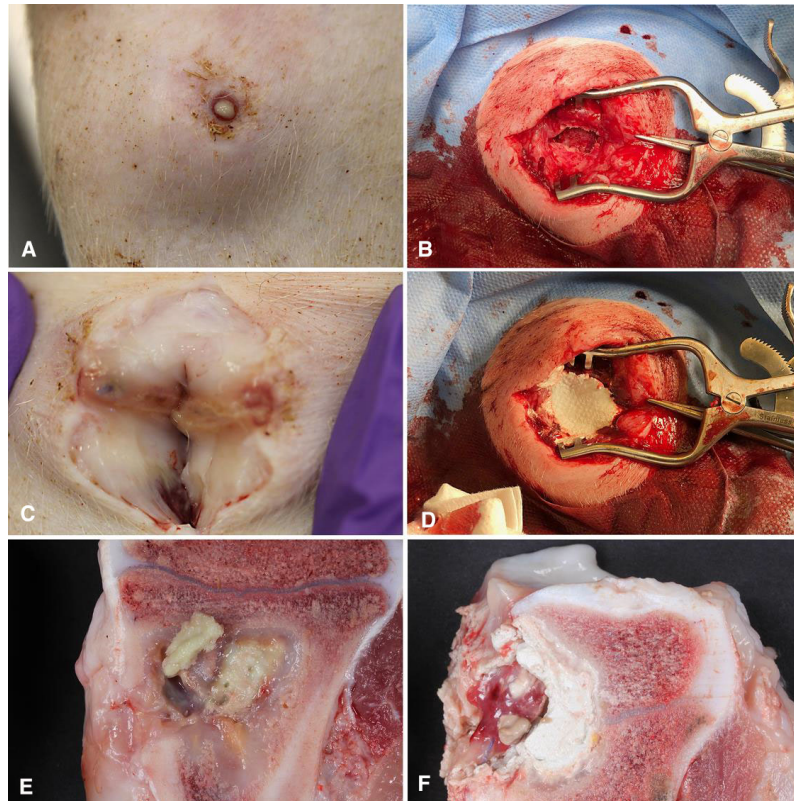


Fig. 15. Porcine model of IAO 19 days after inoculation (left panel). (A, C, E) A skin draining sinus tract surrounded by subcutaneous fibrosis was connected to chronic, purulent, sequestering osteomyelitis. The right panel shows a porcine model of IAO with revision surgery 7 days after inoculation (B, D) and at necropsy 10 days after the revision surgery (F). (B) Bone debridement exposes pinpoint bleeding from vital bone tissue. (D) The bone void created during debridement was filled with a gentamicin eluting degradable biocomposite (as described in Fig. 1). (F) The local administration of gentamicin could not prevent infection, and the biocomposite was surrounded by pus and fibrosis post-mortem.

term subacute implies an inflammatory condition with cell infiltration predominantly involving neutrophils, together with initiation of tissue repair/healing (VIII). Histologically, the PIBA is comparable with the peri-prosthetic type II membrane (i.e. the infectious type), which develops between bone tissue and an infected prosthesis in patients [88]. All animals inoculated with bacteria developed infections in accordance with the diagnostic criteria defined for IAO (see Chapter 1) [16] and PJIs (I–III, V–VIII) [76]. Clinically, the 5-day-old lesions observed in our model would be defined as resulting from early or acute infections [16]. Recent research has shown that the model can be used in studies involving a time frame of 19 days (Fig. 15) [12].

The porcine IAO model corresponds to stage 3A on the Cierny–Mader classification system, that is localized osteomyelitis, usually involving both cortical and medullary bone in a patient without systemic or local compromising factors [18]. In patients, bone infections are very adversely affected by comorbidities such as obesity, diabetes, immune suppression and coagulopathy [4,5,16]. These comorbidities are extremely common in orthopaedic patients, and understanding the impact of these factors is critical. To date, no studies have reported any of these comorbidities in a large animal bone infection model [89]. The relatively minor and limited lesions observed in our porcine model (mean PIBA = 3 mm; I–III, V–VIII) are similar to those reported in patients but

very different from the lesions observed in many rabbit- and rodent-based IAO models, where the entire inoculated bone is often affected.

Moriarty et al. describe the implant that was used in the porcine IAO model as one of low complexity, which corresponds to a non-functional implant or a biomaterial serving as a foreign body (II, III) [34]. However, highly complex models, with biomaterials that correspond to completely functional devices such as hip prostheses, may be unnecessary at the proof of concept stage or in preliminary studies [34]. Experimental implant-associated bone infections involving complex implants may only be required as a technology reaches the late pre-clinical phase (e.g. a new antimicrobial surface coating) [34]. These considerations regarding low and high implant complexity are commensurate with the current application of the porcine IAO model. During the previous 4 years, the model has been used very effectively to develop a novel anti-biofilm compound and a novel antimicrobial surface-coating technique. Moreover, these new successful approaches are to be applied in a more complex and refined version of the IAO model based on insertion of full joint prostheses in mature minipigs.

CHAPTER 4

Application of the porcine IAO model – tissue biofilm

In vivo biofilm – Most of our current information regarding biofilm formation is based on research from *in vitro* models [7]. However, recently several studies have demonstrated that biofilms grown *in vitro* are different from those formed *in vivo*; that is, *in vitro* models are not representative of infection sites (VIII) [7,90]. *In vitro* biofilms consist solely of bacteria and bacterial-derived components, whereas *in vivo* biofilms contain a mixture of bacterial and host-derived elements [7]. Furthermore, *in vivo* biofilms are not continuously provided with fresh media and they are not necessarily attached to an artificial surface, but instead are embedded in tissues [7]. As an example of the impact of the local environment, the maximum diameter of an *in vivo* biofilm is 200 µm (probably due to local oxygen depletion),

whereas an *in vitro* biofilm can reach several centimetres [7]. Bacteria growing in biofilms have low metabolic activity; however, they stimulate an inflammatory reaction, which is hard to replicate in a laboratory setting [91].

Porcine models of biofilm infections in humans

– Recently, porcine models of bacterial biofilm infections in humans were reviewed and the patho-morphology in the models was compared with patho-morphology of the same spontaneous chronic infections in pigs at slaughter (IV). Furthermore, descriptions of lesions in the pigs were compared to those described in patients. In addition to the present IAO model, pigs have also been used to model chronic bacterial diseases that are associated with biofilm formation in humans, such as endocarditis, pyelonephritis and haematogenous osteomyelitis (Fig. 16) [69,70,92]. The primary databases used as information sources for the review were Google Scholar, REX, Web of Science and PubMed (IV). Regardless of the type of infection, the macroscopic patho-morphology of the experimental lesions and lesions from slaughter pigs with spontaneous infections were similar (Fig. 16; IV). In addition, the pathogenesis and pathological descriptions of lesions associated with endocarditis [93,94], pyelonephritis [95,96] and osteomyelitis [1,64] in humans and slaughter pigs were identical. Bacterial aggregates were identified in all the experimental models included in the review; however, only 6 of the 30 studies that were included comment on the formation of biofilm (IV). This is probably because most of the models were established decades ago, and biofilm is a relatively new area of interest in studies of chronic infectious diseases [6]. Biofilm formation is rarely included in descriptions of chronic spontaneous porcine bacterial infections. A study by Costertorn et al. in 2003 observed that all chronic bacterial diseases in humans examined over a 12-year period involved biofilms [97]. In addition, it has been recommended that all refractory chronic bacterial infections in humans should be analysed for the presence of biofilm [98]. Thus, chronic porcine bacterial infections are probably caused by biofilms similar to those described in studies on patients. Therefore, the examination of biofilms associated with chronic infections in farm

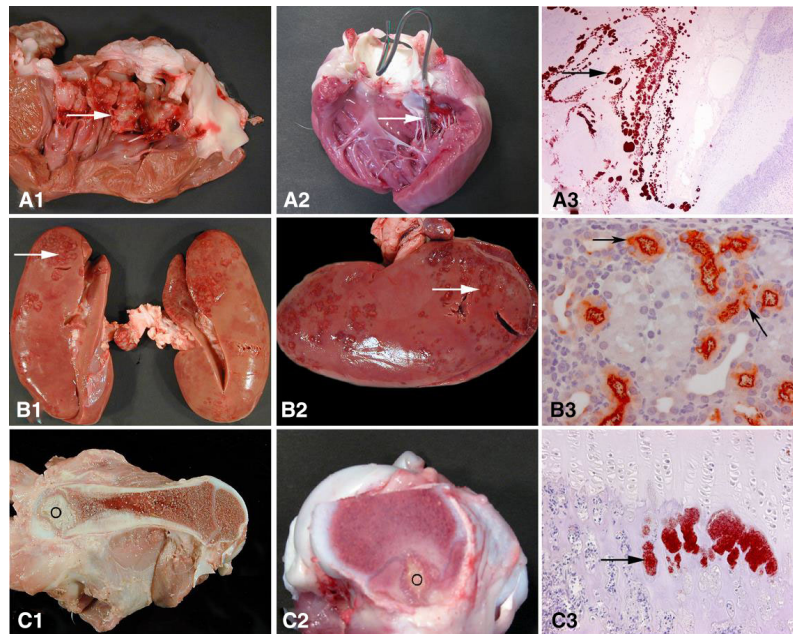


Fig. 16. Comparative patho-morphology of chronic spontaneous bacterial infections in slaughter pigs (left column) and experimental porcine models of the same human infections (middle column). Right column: microscopy of the lesions that are shown in the middle column. Row A: Endocarditis. A1: Left side, thrombotic valvular endocarditis (arrow). A2: A permanent catheter (arrow) is inserted into the left ventricle prior to inoculation of *Staphylococcus aureus* bacteria. A3: IHC staining of *S. aureus* (arrow) on the mitral valve. Row B: Pyelonephritis. B1, B2: Polar lesions resulting from pyelonephritis (arrows) caused by *Escherichia coli*. B3: IHC staining of *E. coli* (arrows) in the proximal tubule. Row C: Haematogenous osteomyelitis. C1, C2: Purulent osteomyelitis (O) in the femur. C3: IHC staining of *S. aureus* (arrow) located in metaphyseal capillary loops (V). [69,70,92]

animals represents a good opportunity to study natural tissue biofilms in general (IV).

Tissue biofilm – For orthopaedic infections, bacteria are usually considered in the context of biofilm formation on an implant surface [99]. However, biofilm formation can also occur within peri-implant tissue when bacteria attach to other bacteria and bone matrix components (II, III, VI) [19,99]. Clinically, the phenomenon of tissue-based biofilms is well documented in case reports describing IAO and other types of chronic infections such as chronic wounds and pneumonia in cystic fibrosis patients [99–101]. Experimentally, tissue-based biofilms have been studied in models of catheter-based infections established in rabbits and mice and the new porcine IAO model (II, III, VI) [102,103]. Studies on the new porcine IAO model showed that after 1 week, the

inoculated bacteria were localized in aggregates that penetrated up to 0.5 cm into the peri-implant tissue from the implant–tissue interface (Fig. 17; II). Furthermore, in the porcine model, no bacterial growth was observed on the tissue surface at the interface (Fig. 17; II). Clearly, drilling the implant cavity and injecting bacteria into the porcine IAO model created a peri-implanted bacterial reservoir (II, III, VI) [99]. As staphylococci are immotile bacteria, bacteria induced tissue destruction such as osteolysis is assumed to contribute to the peri-implant tissue spread. Once located in the peri-implant bone tissue, the infecting bacteria can form biofilms, small colony variants or they can be internalized by osteoblasts, all of which favours persistence of the infection [104–106]. Biofilm formation will lead to increased antimicrobial tolerance, which renders antibiotic treatment less effective [28].

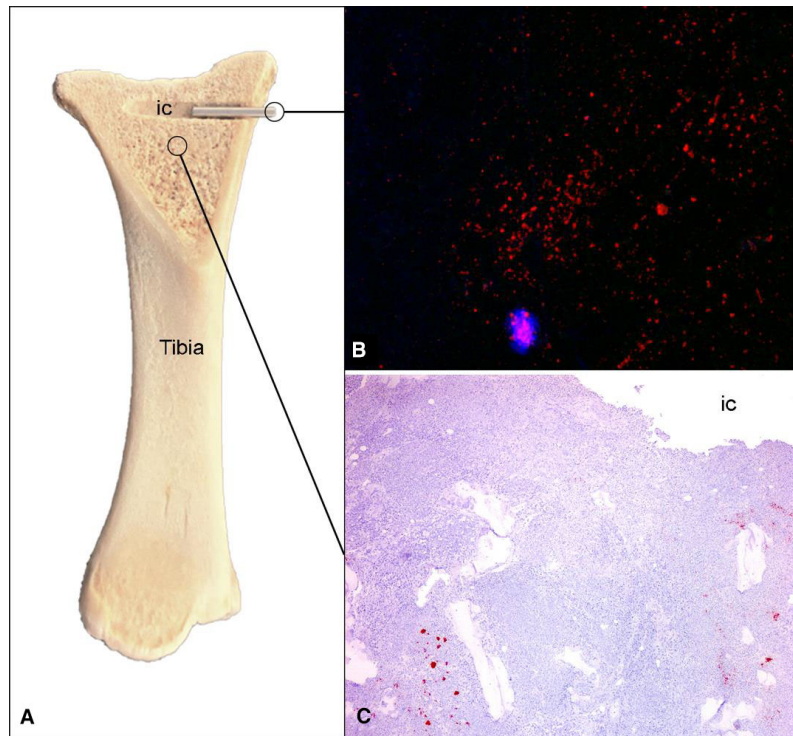


Fig. 17. Porcine model of IAO. (A) An implant cavity (ic) is drilled into the tibial bone, bacteria are injected into the cavity and a steel implant is inserted. The pigs were euthanized after 5 days, and samples were collected to analyse the tissue and assess the colonization of the implant. (B) Red *Staphylococcus aureus* bacteria localized on the implant. Peptide nucleic acid fluorescence in situ hybridization using a specific probe for *S. aureus*. (C) Red *S. aureus* bacteria were localized within the peri-implant tissue at different distances from the implant–tissue interface. Bacterial colonization of the interface (white arrow) was not observed. IHC staining using an antibody specific for *S. aureus* (II).

Therefore, surgical debridement to remove the peri-implant bacterial reservoir is often necessary to eradicate the infection [16].

New staining technique for S. aureus tissue biofilm – Pathologists are often unaware of the presence of tissue biofilms when they examine slides to diagnose bacterial infections in histology laboratories. Commonly, bacteria can be visualized in standard haematoxylin and eosin (HE)- or Gram-stained tissue sections, although one disadvantage of HE staining is that haematoxylin stains all nucleic acids, making it difficult to differentiate bacteria from host cells [107,108]. The extracellular matrix of a biofilm is composed of molecules produced both by the bacteria and the host and includes polysaccharides, proteins,

enzymes, nucleic acids and lipids (Fig. 3) [109]. All of these different molecules have specific roles related to survival and growth of the embedded bacteria [109]. In routine histology laboratories, different HC stains are frequently used to identify the same particular types of molecules, for example Masson staining colours collagen blue [108]. Therefore, a reasonable approach to visualizing the extracellular matrix of tissue biofilms could involve using different HC stains (V). However, although the extracellular matrix is an important element of biofilms, it is unclear which HC stains could be used to identify the matrix components. Therefore, different HC stains, used separately or in combination with IHC techniques to detect *S. aureus*, were applied to tissue sections exhibiting staphylococcal osteomyelitis and the

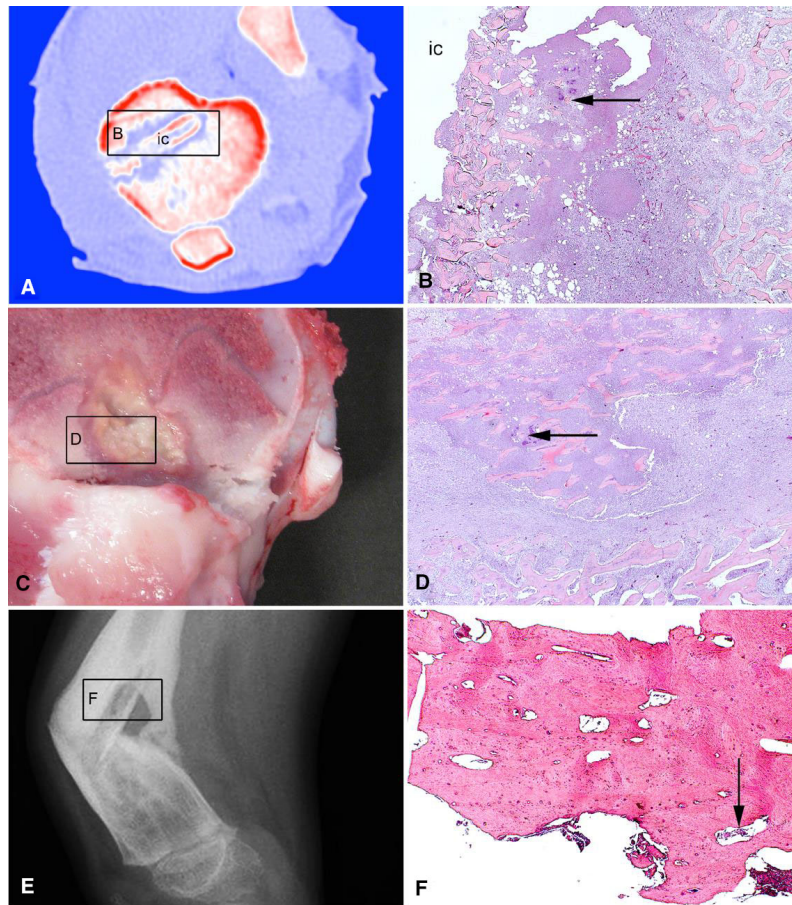


Fig. 18. Bone tissue used to develop a new biofilm staining protocol. (A) Porcine model of IAO (5 days). CT scan showing the tibial implant cavity (ic) used for injection of *S. aureus* and insertion of a small steel implant. (B) Histology of image A showing bacteria (arrow) in the peri-implant tissue adjacent to the implant cavity (ic). HE. (C) Porcine model of haematogenous osteomyelitis euthanized 15 days after inoculation of *S. aureus* into the femoral artery. A lesion found in the right femoral metaphysis is shown. (D) Histology of image C showing bacteria (arrow) in the centre of the lesion. HE. (E) X-ray of a child with chronic haematogenous osteomyelitis and a pathologic fracture of the right femur. (F) Histology of image E showing bacteria (arrow) in a cortical sequestrum. HE (VI).

biofilm matrix was examined using light microscopy (VI).

Sampling of tissue: A block of paraffin-embedded infected bone tissue was obtained from the new porcine IAO model. In addition, a block of infected bone tissue was obtained from the distal femur of a pig inoculated with 10^4 CFU/kg body weight of *S. aureus* (S54F9) into the right femoral artery and euthanized 15 days afterwards [69]. Finally, a block of infected bone tissue was obtained from a 5-year-old boy with chronic haematogenous osteomyelitis of the right femur (Fig. 18; VI) [110]. According to Bjarnsholt et al., this case

fulfilled all the criteria for a chronic biofilm infection, including tissue-adherent bacteria found in clusters (5–200 μM), infection localized to a specific anatomical site, and infection persistence despite exposure to antibiotics [7].

Histochemistry and immunohistochemistry: In total, 25 consecutive tissue sections (4–5 μM) were cut from both blocks of porcine tissue and stained using the HC stains listed in Table 3 (VI). For each stain, the colour of the bacteria and the clarity of the extracellular biofilm matrix were recorded (VI). Furthermore, the level of contrast between the colour of the bacteria and the surrounding tissue was

Table 3. Results of using 25 histochemical stains to visualize bone tissue from porcine models of haematogenous and implant-associated osteomyelitis induced by *Staphylococcus aureus* S45F9. Contrast between bacteria and the matrix: poor (+), fair (++), good (+++). Modified from VI

The colour of biofilm			
Stain	Bacteria colour	Biofilm matrix colour	Contrast
Alkaline congo red	Purple	No	++
Crystal violet	Purple	Yes, Purple	++
Gomori's reticular fibres	Brown/purple	No	+
Luna	Blue	Yes, Blue	+++
Martius scarlet blue	Purple	No	+
Masson trichome	Brown/purple	No	++
Picro-sirius red	Orange	Yes, Orange	++
PTAH	Brown/purple	No	+
Van Gieson	Brown	No	+
Verhoeff's	Purple	No	+
Alcian blue pH1	Blue	Yes, Blue	+
Alcian blue pH3	Blue	Yes, Blue	+++
PAS	Purple	Yes, Purple	++
Safranin O	Purple	Yes, Purple	+++
Toluidine blue-acetone	Blue	Yes, Blue	++
Oil red O	Purple	Yes, Purple	++
Perls' Prussian blue	Red	No	++
Von kossa	Brown	No	+
Alizarin red S	Yellow/brown	No	+ / ++
Giemsa	Blue	Yes, Blue	+++
Grocott methenamine silver	Black	No	++
Levaditis	Black	No	++
Gram	Purple/blue	Yes, Purple/blue	+++
Feulgen nuclear reaction for DNA	Turquoise	No	+
Methyl green-pyronin	Red/pink	Yes, Red/pink	+++

scored: poor contrast (+), fair contrast (++) or good contrast (+++). Six of the 26 HC stains tested displayed the extracellular matrix and showed good contrast (Table 3). Among these six stains, Alcian Blue pH3, Luna and Methyl green-pyronin could be optimally combined with an IHC protocol based on an antibody against *S. aureus* (Fig. 19; VI). This resulted in red to light-brown bacterial cells and a visible extracellular matrix. The three stains were also applied to the human tissue (VI). The light-blue colour of the biofilm matrix visible with Alcian blue pH3 was due to staining of polysaccharides, and the blue and orange colours of the biofilm matrix visible with Luna and Methyl green-pyronin, respectively, were due to staining of nucleic acid (VI). Double staining of *S. aureus* and biofilm matrix was visible in approximately 10% and 80% of the bacterial aggregates in the porcine and human tissue sections, respectively (VI). The double-

stained tissue sections (HC plus IHC stained) were scanned to create digital slides, and image analyses were performed to estimate the proportions of bacterial cells and extracellular matrix in representative aggregates (Fig. 20). This revealed a higher ratio of matrix compared with bacterial cells in the human tissue than in the two porcine models (VI).

According to the European Society for Clinical Microbiology and Infectious Diseases' guidelines for diagnosing biofilm infections, to confirm the presence of a biofilm, tissue microscopy must show evidence of an infective process, such as the presence of leucocytes, and the microorganisms present must form aggregates that are embedded in a matrix which is separate from the surrounding tissue [111]. These requirements were met using the new combination of HC and IHC techniques for visualizing *S. aureus* biofilm under light microscopy (VI).

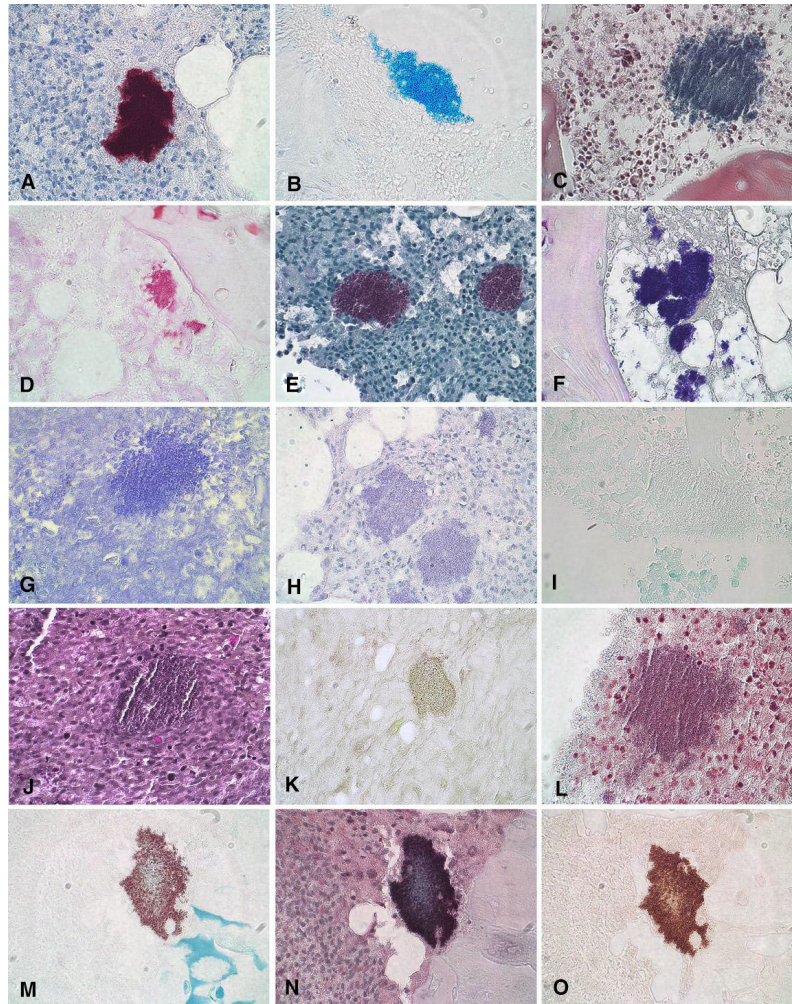


Fig. 19. IHC (A), histochemical (B–L) and combined IHC and histochemical (M–O) staining of *Staphylococcus aureus*-infected porcine bone tissue. (A) *S. aureus* IHC staining, (B) Alcian blue pH3, (C) Luna, (D) Methyl green-pyronin, (E) Safranin O, (F) Gram, (G) Crystal Violet, (H) Oil red, (I) Feulgen, (J) Verhoeff, (K) Alizarin Red, (L) Masson trichrome, (M) Alcian blue pH 3 + *S. aureus* IHC staining, (N) Luna + *S. aureus* IHC staining, (O) Methyl green-pyronin + *S. aureus* IHC staining. All images are the same scale (VI).

CHAPTER 5

Application of the porcine IAO model – antimicrobial agents

Treatment of IAO – Surgery is required to treat almost all IAO cases [16]. Sequestra and tissue biofilms compromise the effect of antibiotic therapy; therefore, drainage, debridement and implant removal are required. After debridement, approximately 2 weeks of intravenous antibiotic therapy is administered to eradicate any biofilm remaining at the infection site [2]. Thereafter, prolonged oral

antibiotic therapy for 6–12 weeks is recommended, depending on the stage of the infection, for example acute, late or delayed [2,16]. However, there is no scientific evidence recommending, nor comparative clinical studies defining, an optimal duration of antimicrobial treatment [16]. Animal models of bone infections are valuable because they can be used to test prophylactic and therapeutic strategies for managing IAO in humans [31]. However, treatment studies using animal models of IAO are complex. If the treatment involves surgical debridement or application of local antibiotics,

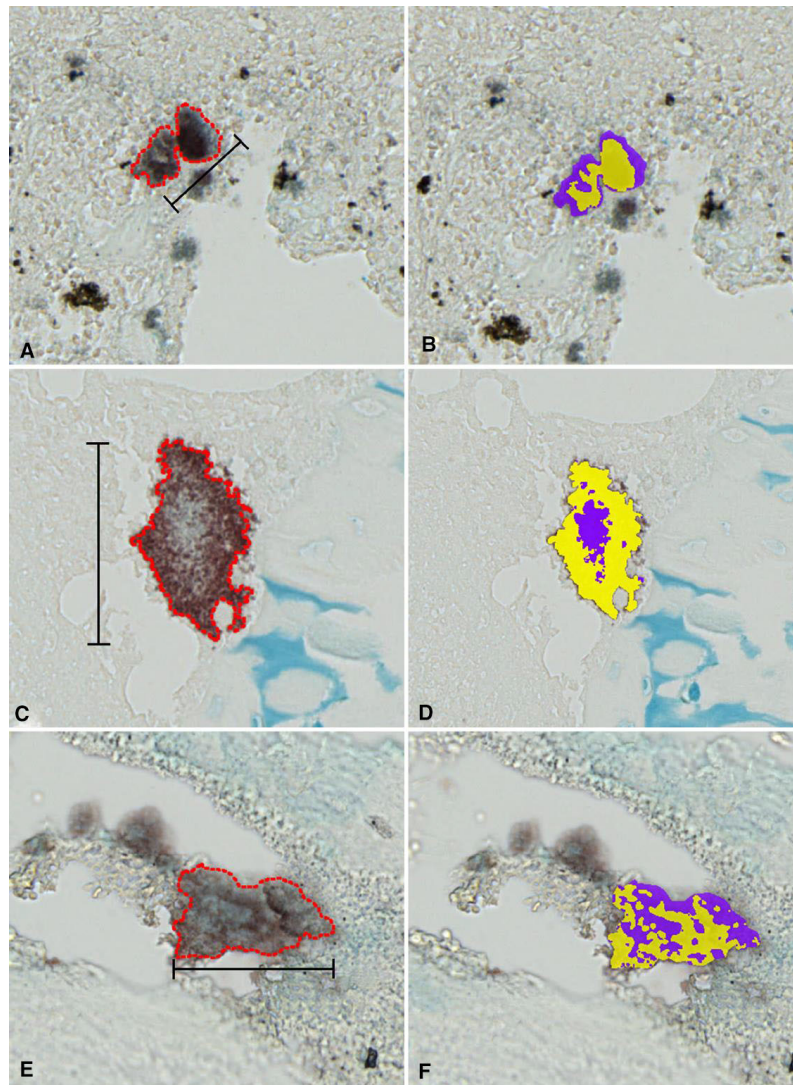


Fig. 20. Proportions of bacteria and extracellular matrix in *Staphylococcus aureus* biofilm infections. Left column: combined IHC staining (for *S. aureus*) and Alcian blue pH3 staining of representative bacterial biofilms (red outline) displaying both bacteria (red/brown) and extracellular matrix (blue). Right column shows the colours used for image analyses: yellow = bacterial cells; purple = extracellular matrix. (A and B) Bone tissue from a porcine model of *S. aureus* IAO infected for 5 days. Scale bar = 40 μm . (C and D) Bone tissue from a porcine model of *S. aureus* haematogenous osteomyelitis infected for 15 days. Scale bar = 78 μm . (E and F) Bone tissue from a patient who had *S. aureus* haematogenous osteomyelitis for more than 1 year. Scale bar = 72 μm (IV).

then at least two surgical procedures are required (I, VII) [31]. One procedure is required to inoculate the animals and after the infection has developed, a second surgical treatment procedure is necessary [31]. Similarly, preclinical treatment studies based on the administration of systemic antibiotics also require infections to develop before treatment can be initiated (I, VII). In contrast, a shorter

infection period is used for animals in prophylaxis studies because anti-infective approaches are applied before or together with bacterial inoculation and only one surgical procedure is needed (VIII).

Antimicrobial pharmacokinetics in infected bone tissue – Successful systemic antimicrobial treatment of IAO depends on using drugs that can

penetrate the target site and have proven effectiveness against the invading pathogen. Adequate bone penetration is important because antibiotics need to reach a particular concentration at the infection site to kill pathogens and prevent the development of antibiotic resistance. Bone infection treatment failure may be partly due to lack of knowledge regarding target-site penetration of systemically administered antimicrobial agents (I, VII) [112,113]. For many antimicrobial agents, plasma pharmacokinetic targets have been identified, whereas tissue targets have not [114]. Bone is less vascularized than other tissues, and recent studies involving animals and humans have revealed reduced bone penetration of intravenously administered antibiotics that are frequently used to treat orthopaedic conditions [115,116]. Therefore, antimicrobial treatment regimens that are based on pharmacokinetic studies of plasma may be more

susceptible to therapeutic failure. Patients with IAO may have impaired blood circulation at the infection site, and certain aspects of pathology (e.g. fibrosis, sequestra and suppuration) may further reduce the penetration of antibiotics (I, VII) [1]. Thus, the pharmacokinetic characteristics of antimicrobial agents applied to normal healthy bone tissue may not be the same as those of the same agents applied to infected bone tissue. Recently, the impact of bone infection and inflammation on tissue penetration was investigated in the porcine model of IAO (I, VII). In these studies, pigs with IAO for 5 days were anaesthetized and microdialysis (MD) catheters were placed in the infected implant cavities, in the infected bone tissue 1 cm from the implant cavities, and in the associated infected soft tissue (I, VII). In addition, MD catheters were placed in the bone and overlying soft tissue of the contralateral healthy leg (Fig. 21A–C). In two

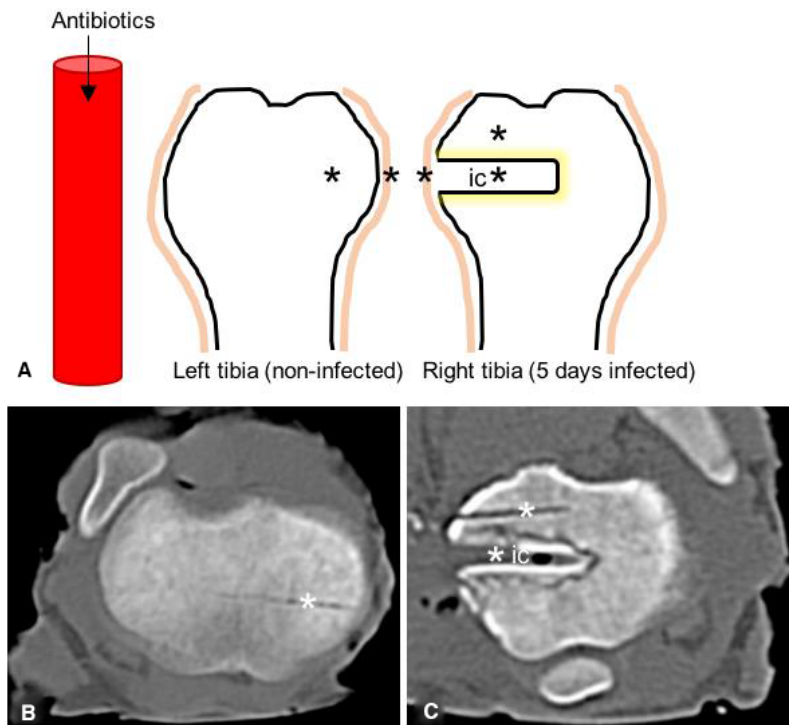


Fig. 21. Penetration of antimicrobial agents into infected bone tissue following intravenous administration in a porcine model of IAO. (A) Microdialysis (MD) catheters (*) were placed in healthy and infected subcutaneous tissue, healthy and infected trabecular bone, and within the infected implant cavity (ic). The antimicrobial agents were administered intravenously and samples were subsequently collected from plasma and the five MD catheters every 30 min for 8 h. (B and C) CT scans showing the implant cavity and the drilled cavities for the MD catheters (*) in healthy and infected bone tissue (VII).

separate studies, a single dose of either cefuroxime or vancomycin was administered intravenously and samples were taken from plasma and the five MD catheters regularly over an 8-h period (I, VII). Previously, antimicrobial penetration into bone tissue has been investigated using surgically collected bone specimens, from which the administered antimicrobial agents were subsequently extracted and quantified [117]. However, MD offers an attractive alternative to using bone samples because it can be used to selectively measure the unbound extracellular fraction of antibiotics over time [118]. Briefly, MD is a minimally invasive technique based on small catheters with semipermeable membranes at the tip [118]. The semipermeable membranes allow diffusion (dialysis) of solutes between the extracellular fluid and the perfusate in the catheter [118]. Because the catheter is continuously perfused with isotonic saline, an equilibrium is never reached [118].

The measured concentration profiles of cefuroxime and vancomycin showed that penetration of these antibiotics into the infected implant cavity (AUC_{0-last} and C_{max}) was significantly impaired (I, VII). For cefuroxime, penetration into infected trabecular bone was also impaired, but impairment of penetration into the implant cavity was more marked (I). Vancomycin penetration into infected trabecular bone was impaired compared to its penetration into healthy bone (VII). In general, cefuroxime penetration of various tissues was better than that of vancomycin. Therefore, both the sensitivity of the infecting pathogen to a particular drug and the drug's specific bone tissue pharmacokinetic profile should be considered when selecting appropriate antimicrobial agents to treat IAO (I, VII). Consequently, more aggressive antimicrobial treatment regimes for bone infections should be developed and tested to secure sufficient target-site exposure.

Histopathology associated with reduced antimicrobial penetration – Because of the results of the pharmacokinetic studies in the porcine IAO model, it was decided to characterize the histological changes associated with reduced antimicrobial penetration (V). Paraffin-embedded tissue blocks containing

longitudinal sections of the implant cavity, which showed pathological changes surrounded by healthy tissue, were sampled from all animals (V). HE-stained sections were used to confirm that all animals were infected, in accordance with the Feldman criteria (i.e. more than five neutrophils per HPF, after evaluating five HPFs) [80]. The thickness of the pathological tissue (i.e. the PIBA) was measured as previously described in Chapter 3. The PIBA measurements ranged from 1.2 to 3.8 mm, and greater PIBA thickness was significantly correlated with reduced antimicrobial penetration, that is low AUC_{0-last} and C_{max} (V). Thus, reduced penetration of systemically administered antimicrobial agents into tissue surrounding infected implants was correlated with the progression of bone pathology (V). In particular, PIBAs that were >3 mm thick showed significant reductions in antimicrobial agent penetration (Fig. 22; V). The three largest foci within a PIBA that had no obvious vessels were identified and outlined (V). The areas of these three vessel-free foci were calculated (range, 5.2–17.6 mm²), and the foci comprised osteonecrotic tissue, inflammatory cells, bacteria and bands of collagen (V). Morphological examinations and IHC analyses targeting von Willebrand factor were used to identify small arterioles and veins, blood-filled capillaries and regions undergoing angiogenesis. The PIBAs contained all of these vessel types and morphological characteristics (V). Premature granulation tissue with blood-filled capillaries was primarily observed at the periphery of implant cavities but was occasionally contiguous with a cavity. In general, thrombosis was not observed within or outside PIBAs. In order to collect systemically administered cefuroxime from the MD catheters (i.e. from the extracellular fluid) the drug must have spread and crossed the capillary endothelia inside the PIBAs [119]. However, despite the presence of capillaries close to the implant cavities, decreased penetration was observed (V). Therefore, either the capillaries were unable to compensate for the vessel-free foci or blood flow within the capillaries had decreased. Increased intramedullary pressure and stasis could have decreased the local blood flow. After escaping from the capillaries,

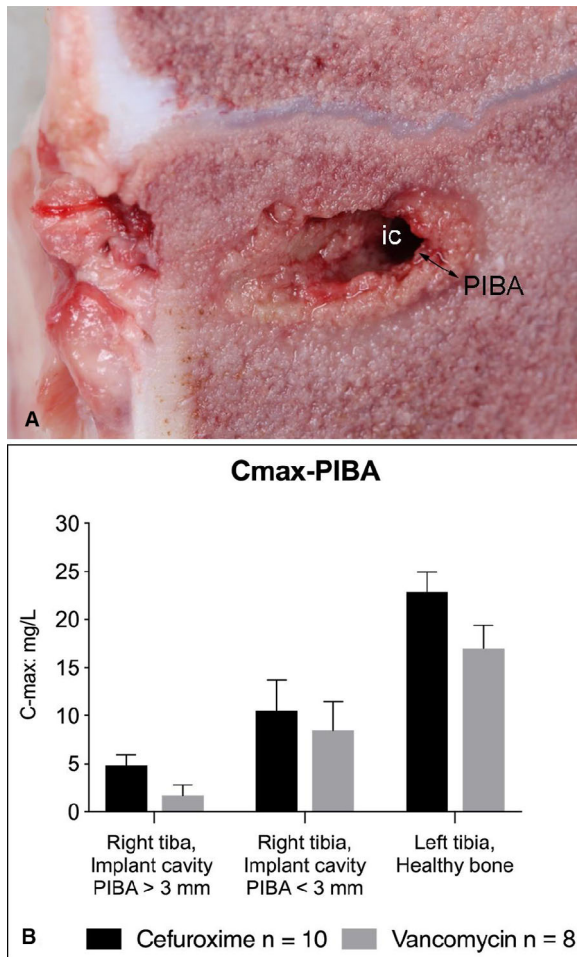


Fig. 22. Results of antimicrobial (vancomycin and cefuroxime) penetration into healthy bone tissue and the infected implant cavity in a porcine model of IAO (study set up, see Fig. 21). (A) A PIBA surrounds the implant cavity (ic). (B) The y-axis shows the maximal measured antimicrobial concentration (C-max). Data from the infected implant cavity were separated into two categories based on PIBA size (PIBA < 3 mm and PIBA > 3 mm). If the PIBA extended more than 3 mm into the bone tissue, a dramatic reduction in antimicrobial penetration was observed (V).

cefuroxime could only enter the MD catheter in the implant cavity by diffusion through the interstitial fluid [119]. Therefore, diffusion may have been impaired by the suppurative inflammatory response, increasing the viscosity of the interstitial fluid (V) [120]. Furthermore, bone destruction may have enlarged the

implant cavity, increasing the distance that had to be covered by diffusion (V) [119].

Local antibiotic treatment of bone infections – Because mature biofilms can develop antimicrobial tolerance of more than 1000 times the minimum inhibitory concentration (MIC) value and antimicrobial agents have difficulty penetrating infected bone tissue, surgical eradication of dead bone tissue and biofilm is mandatory for successful treatment of CO [16]. However, after debridement the bone should be considered contaminated with disseminated bacteria released during surgery [121]. The bone surface will be covered in haematomas, and the local environment will be low in oxygen and will have a low pH, providing an ideal environment for new biofilms to form from the disseminated bacteria [121]. Systemic antibiotics should be administered to target these remaining bacteria [2,16,121]. Another option is to use a local antibiotic carrier that can fill the bone void and deliver high concentrations of local antibiotics to the surrounding tissue [2,121]. One of the clear advantages of using local antibiotics is that this can achieve high local antibiotic concentrations, avoiding the risk of systemic toxicity [2,121]. Research has demonstrated that local antibiotic carriers can elute 10–100 × the MIC value of the most common organism involved in IAO [122,123]. However, the extent to which locally applied antibiotics can penetrate into the surrounding bone tissue remains unclear. Recently, the porcine IAO model was used to investigate the microbiological impact of a gentamicin-loaded bone void filler, without simultaneous systemic antibiotic treatment, following limited or extensive debridement of osteomyelitis lesions [12]. Regardless of the type of debridement used, the bone void filler was contaminated with biofilm 10 days after revision surgery. However, significantly less surrounding bone inflammation was present in cases of extensive debridement [12]. Consequently, the bone tissue concentrations of gentamicin obtained from the bone void filler may have been too low to eradicate the remnants of the mature biofilms left behind after debridement, allowing the carrier product to be colonized [12]. The study measured only low concentrations

of gentamicin in the surrounding bone tissue, which supports this interpretation [12].

The most frequently used local antibiotics are gentamicin, tobramycin, vancomycin and cephalosporins [124]. The antibiotic bone void filler or carrier may be resorbable or non-resorbable [121]. Positive treatment outcomes have recently been reported in different retrospective clinical studies of resorbable antibiotic carriers [125]. Regardless of the local antimicrobial carrier used, investigators must understand the partitioning of antibiotics within the bone void and the surrounding debrided/infected bone tissue once released from the carrier. The effect of local antibiotics will depend on the antibiotic release profile from the carrier, tissue penetration and the impact of host-specific factors such as bleeding and inflammation. These factors may influence antimicrobial agent concentrations and diffusion characteristics, thereby having an effect on the susceptibility of pathogens to the treatment (VIII).

In vivo susceptibility to gentamicin – The impact of particular *in vivo* factors was recently investigated using the novel porcine IAO model (VIII). The aim of the study was to set up an *in vivo* single-dose antimicrobial susceptibility test for biofilm prevention by adding different concentrations of gentamicin to the inoculum introduced into the porcine IAO model.

Prior to *in vivo* testing, an *in vitro* time-kill curve was generated using different gentamicin concentrations (16, 160, 1600, 16,000 and 160,000 \times MIC) and the *S. aureus* strain used for inoculation (MIC = 0.25). After 24 h, only the positive control (no gentamicin) and the sample containing 16 \times MIC had a viable bacterial count. For the high MIC values (16,000 and 160,000), the detection limit was reached within 2 h, and for the low MIC values (160 and 1600), the detection limit was reached within 4 h (VIII). Mixing the bacteria and gentamicin concentrations described above for 60 s, as was performed before inoculation of the porcine IAO model, did not neutralize the inoculum. A total of 25 pigs were included in the study. Pigs inoculated with saline (Group A) or bacteria (Group B) were historic controls from previous experiments (II, III). An additional four groups (Groups C–F) were

included to test different doses of gentamicin (VIII). The implant cavity in the model was created as previously described (III); however, 1 min before inoculation, different doses of gentamicin were added to the inoculum. The final gentamicin concentrations in the inoculum were 160, 1,600, 16,000 and 160,000 \times MIC (VIII). All pigs were euthanized 5 days after inoculation and analysed using the methods described in Chapter 3. The bactericidal effect of gentamicin was evaluated using microbiological swabs of the implant cavity, sonication of implants and IHC staining of *S. aureus* within the PIBAs. No bactericidal effect was observed for gentamicin concentrations of 160 and 1600 \times MIC (VIII). In contrast, bactericidal effects were observed for gentamicin doses of 16,000 and 160,000 \times MIC (the high MIC value group; VIII). A significant reduction in the number of bacteria attached to the implant surface was only observed when sonication results from the high MIC value group and Group B (bacteria only) were compared. The microbiological results were consistent with the pathological findings. Macroscopic signs of infection were not observed in saline-inoculated animals or in the high MIC value group (except for one animal with pus in the implant cavity). Pus was found in the implant cavities of all Group B animals and in the implant cavities of low MIC value groups (160 and 1600 \times MIC). Histologically, PIBA measurements and NG counts from the high MIC value group and the group receiving 1600 \times MIC were comparable to those of animals inoculated with saline (VIII). In conclusion, 1600 \times the MIC value of gentamicin must be included in the inoculum of the porcine IAO model to prevent bacterial attachment to the implant (VII). However, when only the bone tissue was considered, all concentrations $>$ 160 \times MIC resulted in a tissue response comparable to saline inoculation (VIII). All the gentamicin doses tested were 100% effective *in vitro* against the planktonic form of the *S. aureus* strain. However, after inoculation, only high doses ($>$ 1000 \times MIC) retained sufficient bactericidal effects, regardless of the inflammatory reaction and the onset of biofilm formation on the implants (VIII). Pre-inoculation mixing of the inoculum

ensured optimal, equal, and reproducible contact between bacteria and gentamicin within the tissue (i.e. bactericidal effects were based on exposure to a single antibiotic dose and the influence of specific *in vivo* factors).

Drilling the implant cavity resulted in an acute inflammatory response within the surrounding bone tissue. In addition, bacterial inoculation induced further acute inflammation within hours. Acute inflammation leads to vasodilatation and increased vascular permeability, allowing fluid and plasma proteins to enter the cavity [126]. These events may have diluted the gentamicin and coated the implant and surrounding dead bone tissue (produced by drilling the implant cavity) with plasma proteins (Fig. 23). *S. aureus* biofilms start to form on artificial surfaces when bacterial surface molecules bind to plasma proteins attached to the artificial surface [23]. Therefore, biofilms begin to form immediately after inoculation due to bacterial attachment to plasma proteins covering implants and necrotic bone tissue (Fig. 23). Thus, the initiation of biofilm formation may have increased the tolerance of inoculated *S. aureus* bacteria shortly after inoculation (VIII). In addition, tolerance would be enhanced by the acidic inflammatory environment because low pH values increase

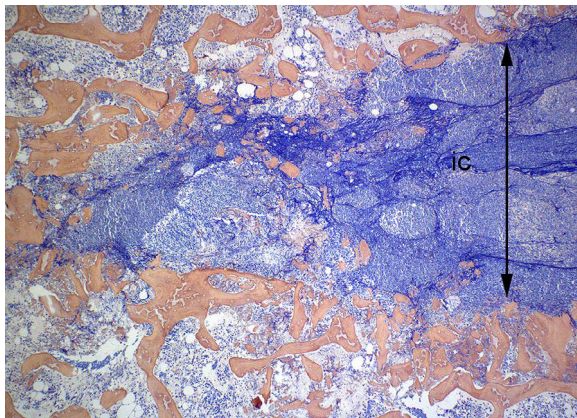


Fig. 23. Porcine model of IAO. An implant cavity (ic) is drilled into the tibial bone, a bacterial inoculum is delivered into the cavity and a steel implant is inserted. A histological image was recorded 8 h after drilling the implant cavity. The implant cavity was filled with blue fibrin threads, which favour bacterial attachment and biofilm formation. Phosphotungstic acid haematoxylin stain.

the MICs of aminoglycosides for gram-positive cocci [127]. The particular doses used in the susceptibility study are clinically arbitrary; however, they demonstrate that the effective doses of locally administered antimicrobial agents must be higher than assumed due to the influence of the local inflammatory environment. Thus, infectious disease specialists and orthopaedic surgeons need to be aware of the fact that the *in vivo* effectiveness and pharmacokinetics of locally administered antimicrobial agents currently is limited.

CHAPTER 6

Conclusions and perspectives

Orthopaedic implants are associated with a high risk of bone infections, which involve biofilm development. For this reason, and due to the increasing prevalence of antimicrobial resistance, there is a clear need for improved diagnostic, preventive and therapeutic technologies to manage bone infections. The pathway to clinical implementation of any anti-infective technology begins with preclinical testing in animal models. This dissertation describes the development, characterization and application of a porcine IAO model, and based on the main results of publications I–IX, the following conclusions were reached:

- An effective and reproducible porcine model of IAO in humans was developed. Insertion of a steel implant and inoculation with 10^4 CFU of *S. aureus* (S54F9) into a pre-drilled tibial bone cavity resulted in an infection rate of 100%.
- Bone infections in the porcine IAO model can be objectively quantified using CT-volume calculations and by assessing neutrophil infiltration, observing histological changes and estimating the number of bacteria attached to the bone implant.
- In many previous studies that used non-rodent large animal models of bone infections, experimental design was poorly reported, methods were of poor quality and the pathological and microbiological parameters used varied significantly.
- Osteomyelitis in slaughter pigs displays similarities to bone infections in patients and

- represents an unexplored resource for investigating biofilm infections.
- Bacterial aggregates occur up to 6 mm deep within the surrounding bone tissue less than 1 week after inoculation. Therefore, peri-implanted bone tissue can serve as a bacterial reservoir shortly after surgery.
 - A combination of HC and IHC techniques can simultaneously stain both the extracellular matrix and the bacteria within a biofilm, using two different colours. Furthermore, there was a positive correlation between the quantity of extracellular matrix in a tissue biofilm and the duration of the infection period.
 - Systemically administered antimicrobial agents showed significantly less penetration into the tissue surrounding infected bone implants than into healthy bone tissue. Different types of antimicrobial agents had different penetration profiles. Therefore, to select an appropriate treatment regime, target-site penetration of an antimicrobial agent must be considered alongside its effectiveness against the infecting pathogen.
 - The quantity of infected bone tissue was negatively correlated with the penetration of systemically administered antimicrobial agents. A PIBA of more than 3 mm results in significantly less penetration of antimicrobial agents.
 - The *in vivo* susceptibility of bacteria to locally administered intraosseous gentamicin is significantly affected by the extent of both inflammation and biofilm development.

Progress in medicine has been accomplished using experimental animals. In total, 90% of the Nobel prizes in 'Physiology or Medicine' have been awarded to investigations based on research with animal models, for example the transmission and treatment of tuberculosis by R. Koch (1905; using guinea pigs, mice and rats), the discovery of insulin by F. Banting and J. MacLeod (1923; using cattle, dogs, fish, pigs and rabbits) and the invention of CT by G. Hounsfield and A. Cormack (1979; using pigs) [30]. Currently, our understanding of the diagnosis, pathology and treatment of many complex diseases may benefit from research on living organisms [30]. One such disease is bone infections. This dissertation describes a reliable and effective porcine IAO model for bone

infection research and demonstrates its almost unlimited applicability for future studies. This porcine IAO model is being used in several ongoing and upcoming national and international projects. The large bone size and potential for comprehensive characterization of bone tissue means that the model may be implemented in studies that could herald a new bone implant era. This may include the development of implants with bio-sensing, self-awareness and self-repair capabilities, for example autonomous implants which may detect developing infections by monitoring the surrounding pH value, oxygen level, temperature or the presence of specific cytokines and respond by releasing antimicrobial agents. Furthermore, studies targeting the development of personalized and multifunctional 3-dimensional printed scaffolds that may be used as bone implants are also in progress. Such implants may be inserted into bone defects caused by infections, in accordance with the needs of individual patients. These implants will be designed to resist infection and enhance osseointegration, promoting rapid recovery and restoring a patient's quality of life.

One approach to treating bone infections could involve preventing bacteria from becoming established within biofilms by developing anti-biofilm compounds. In theory, anti-biofilm compounds could be combined with antimicrobial agents to kill planktonic bacteria before they become embedded in a protective biofilm. This strategy has already benefitted patients with lung infections caused by cystic fibrosis. The porcine IAO model has previously been used to screen novel anti-biofilm compounds isolated from micro-algae (NoMorFilm no. 634588). In addition, large international and multidisciplinary studies have been planned, which will focus on isolating new anti-biofilm compounds from collections of arctic algae and bacteria.

REFERENCES

1. Lew DP, Waldvogel FA. Osteomyelitis. *Lancet*. 2004;364:369–79.
2. Metsemakers WJ, Kuehl R, Moriarty TF, Richards RG, Verhofstad MHJ. Infection after fracture fixation: current surgical and microbiological concepts. *Injury*. 2018;49:511–22.

3. Zimmerli W. Introduction. In: Zimmerli W, editor. Bone and joint infections from microbiology to diagnosis and treatment. Oxford: Jhon Wiley & Sons, Inc; 2015. p. 1–3.
4. Lipsky BA, Aragón-Sánchez J, Diggle M, Embil J, Kono L, Lavery L, et al. IWGDF guidance on the diagnosis and management of foot infections in persons with diabetes. *Diabetes Metab Res Rev.* 2016;32:45–74.
5. Hoffstad O, Mitra N, Walsh J, Margolis DJ. Diabetes, lower-extremity amputation, and death. *Diabetes Care.* 2015;38:1852–7.
6. Bjarnsholt T. The role of bacterial biofilms in chronic infections. *APMIS Suppl.* 2013;121:1–58.
7. Bjarnsholt T, Alhede M, Alhede M, Eickhardt-Sørensen SR, Moser C, Kühl M, et al. The in vivo biofilm. *Trends Micro.* 2013;21:466–74.
8. Blair JMA, Webber MA, Baylay AJ, Ogbolu DO, Piddock LJV. Molecular mechanisms of antibiotic resistance. *Nat Rev Microbiol.* 2015;13:42–51.
9. Calabro L, Richards RG, Moriarty TF. Pre-clinical models of infection in bone and joint surgery. In: Zimmerli W, editor. Bone and joint infections from microbiology to diagnosis and treatment. Oxford: Jhon Wiley & Sons, Inc; 2015. p. 39–54.
10. Lüthje FL, Skovgaard K, Jensen HE, Jensen LK. Pigs are useful for the molecular study of bone inflammation and regeneration in humans. *Lab Anim.* 2018;52:630–40.
11. Lüthje FL, Blirup-Plum SA, Møller NS, Heegaard PMH, Jensen HE, Kirketerp-Møller K, et al. The host response to bacterial bone infection involves a local upregulation of acute phase proteins. *Immunobiology.* 2019;225:151914.
12. Blirup-Plum SA, Bjarnsholt T, Jensen HE, Kragh KN, Aalbæk B, Gottlieb H, et al. Pathological and microbiological impact of a gentamicin loaded bio-composite following limited or extensive debridement in a porcine model of osteomyelitis. *J Bone Res.* 2020;9:394–401.
13. Lüthje FL, Skovgaard K, Jensen HE, Blirup-Plum SA, Henriksen NL, Aalbæk B, et al. RANKL is not regulated during chronic osteomyelitis in pigs. *J Comp Path.* 2019;179:7–24.
14. Walter G, Kemmerer M, Kappler C, Hofmann R. Treatment algorithms for chronic osteomyelitis. *Dtsch Arztebl.* 2012;14:257–64.
15. Darouiche RO. Treatment of infections associated with surgical implants. *N Eng J Med.* 2004;350:1422–9.
16. McNally M, Sendi P. Implant-associated osteomyelitis of long bones. In: Zimmerli W, editor. Bone and joint infections from microbiology to diagnosis and treatment. Oxford: Jhon Wiley & Sons Inc; 2015. p. 303–23.
17. Lito S, Lomessy A, Vaduaux P, Uckay I. Chronic osteomyelitis in adults. In: Zimmerli W, editor. Bone and joint infections from microbiology to diagnosis and treatment. Oxford: Jhon Wiley & Sons Inc; 2015. p. 257–72.
18. Cierny G, Mader JT, Penninck JJ. A clinical staging system for adult osteomyelitis. *Clin Orthop Relat Res.* 2003;414:7–24.
19. Calhoun JH, Manring MM, Shirtliff M. Osteomyelitis of the long bones. *Semin Plas Surg.* 2009;23:59–72.
20. Olson EJ, Carlson CS. Bone, joints, tendons, and ligaments. In: Zachary JF, editor. Pathologic basis of veterinary disease. 6th ed. St Louis, MO: Elsevier; 2017. p. 954–1009.
21. Sheehy SH, Atkins BA, Bejon P, Byren I, Wylie D, Athanasou NA, et al. The microbiology of chronic osteomyelitis: prevalence of resistance to common empirical anti-microbial regimens. *J Infect.* 2010;60:338–43.
22. Zimmerli W. Periprosthetic joint infection: General aspects. In: Zimmerli W, editor. Bone and Joint Infections from Microbiology to Diagnosis and Treatment. Oxford: Jhon Wiley & Sons, Inc; 2015. p. 113–30.
23. McCourt J, O'Halloran DP, McCarthy H, O'Gara JP, Geoghegan JA. Fibronectin-binding proteins are required for biofilm formation by community-associated methicillin-resistant *Staphylococcus aureus* strain LAC. *FEMS Microbiol Lett.* 2014;353:157–64.
24. Kwiecinski J, Kahlmeter G, Jin T. Biofilm formation by *Staphylococcus aureus* isolates from skin and soft tissue infections. *Curr Microbiol.* 2015;70:698–703.
25. Bay L, Kragh KN, Eickhardt SR, Poulsen SS, Gjerdrum LMR, Ghathian K, et al. Bacterial aggregates established at the edges of acute epidermal wounds. *Adv Wound Care.* 2018;7:105–13.
26. Burmølle M, Thomsen TR, Fazli M, Dige I, Christensen L, Homøe P, et al. Biofilms in chronic infections - a matter of opportunity - Monospecies biofilms in multispecies infections. *FEMS Immunol Med Microbiol.* 2010;59:324–36.
27. Costerton JW, Stewart P, Greenberg EP. Bacterial biofilms: a common cause of persistent infections. *Science.* 1999;284:1318–22.
28. Mottola C, Matias C, Mendes JJ, Melo-Christino J, Tavares J, Cacaco-Silva P, et al. Susceptibility patterns of *Staphylococcus aureus* biofilms in diabetic foot infections. *BMC Microbiol.* 2016;119:1–9.
29. Ciampolini J, Harding KG. Pathophysiology of chronic bacterial osteomyelitis. Why do

- antibiotics fail so often? *Postgrad med J*. 2000;76:479–83.
30. Reitmaier S, Graichen F, Shirazi-Adl A, Schmidt H. Separate the sheep from the goats. *J Bone J Surg Am*. 2017;99:1–11.
 31. Calabro L, Lutton C, Din AFSE, Richards RG, Moriarty TF. Animal models of orthopaedic implant-related infections. In: Moriarty FT, editor. *Biomaterials associated infections: immunological aspects and antimicrobial strategies*. New York: Springer Science+Business Media; 2013. p. 273–304.
 32. Elek SD, Conen PE. The virulence of *Staphylococcus pyogenes* for man; a study of the problems of wound infection. *Br J exp pathol*. 1957;38:573–86.
 33. Osmon DR, Berbari EF, Berendt AR, Lew D, Zimmerli W, Steckelberg JM. Executive summary: diagnosis and management of prosthetic joint infection: Clinical practice guidelines by the Infectious Diseases Society of America. *Clin Infect Dis*. 2013;56:1–10.
 34. Moriarty FT, Harris LG, Mooney RA, Wenke CJ, Riool M, Zaat AS, et al. Recommendations for design and conduct of preclinical in vivo studies of orthopaedic device-related infections. *J Orthop Res*. 2019;37:271–9.
 35. Sena E, Wheble P, Sandercock P, Macloed M. Systematic review and meta-analysis of the efficacy of tirilazad in experimental stroke. *Stroke*. 2007;38:388–94.
 36. Currie LG, Delany A, Bennett MI, Dickenson AH, Egan K, Vesterinen HM, et al. Animal models of bone cancer pain: systemic review and meta-analysis. *Pain*. 2013;154:917–26.
 37. Jensen LK, Henriksen NL, Jensen HE. Guideline for porcine models of human bacterial infections. *Lab Anim*. 2019;53:125–36.
 38. Maurens F, Summerfield A, Nauwynck H, Safi L, Gerdt V. The pig: a model for human infectious diseases. *Trends Microbiol*. 2012;1:50–7.
 39. Swindle MM, Makin A, Herron AJ, Clubb FJ, Frazier KS. Swine as models in biomedical research and toxicology testing. *Vet Pathol*. 2012;2:344–56.
 40. Swindle MM, Smith AC, Laber-Laird K, Dungan L. Swine in biomedical research: Management and models. *ILAR J*. 1994;1:1–5.
 41. Harris DL, Alexander TJL. Methods of disease control. In: Taylor DJ, Mengeling WL, Dállaire SY, Straw BE, editors. *Diseases of Swine*. Iowa: Iowa State University Press; 1999.
 42. Martiniakova M, Grosskopf B, Omelka R, Vondrakova BM. Differences among species in compact bone tissue microstructure of mammalian skeleton: Use of a different function analysis for species identification. *J Forensic Sci*. 2006;51:1235–9.
 43. Reichert JC, Saifzadeh S, Wullschlegler ME, Epari DR, Schültz M, Duda GN, et al. The challenge of establishing preclinical models for segmental bone defect research. *Biomaterials*. 2009;30:2149–63.
 44. Reinwald S, Burr D. Review of nonprimate, large animal models for osteoporosis research. *J Bone Miner Res*. 2008;23:1353–68.
 45. Wancket LM. Animal models for evaluation of bone implants and devices: comparative bone structure and common model uses. *Vet Pathol*. 2015;55:842–50.
 46. Pearce AI, Richards RG, Milz S, Schneider E, Pearce SG. Animal models for implant biomaterial research in bone: a review. *Eur Cells Mater*. 2007;13:1–10.
 47. Aerssens J, Boonen S, Lower G, Dequekker J. Interspecies differences in bone composition, density, and quality: potential implications for in vivo bone research. *Endocrinology*. 1997;139:663–70.
 48. Dawson HD. Genetics and immunology. In: McAnulty PA, Dayan AD, Ganderup NC, Hastings KL, editors. *The minipig in biomedical research*. Great Britain: CRC Press; 2011. p. 323–42.
 49. Legrand N, Ploss A, Balling R, Becker PD, Borsotti C, Brezillon N, et al. Humanized mice for modelling human infectious diseases: challenge, progress, and outlook. *Cell Host Microbe*. 2009;6:5–9.
 50. Nishitani K, Bello-Irizarry SN, Bentley KLM, Daiss J, Schwarz EM. The role of the immune system and bone cells in acute and chronic osteomyelitis. In: Lorenzo J, Horowitz M, Choi Y, Takayanagi H, Schett G, editors. *Osteoimmunology*. St Louis, MO: Elsevier; 2011. p. 283–95.
 51. Seok J, Warren HS, Cuenca AG, Mindrinos MN, Baker HV, Xu W, et al. Genomic responses in mouse models poorly mimic human inflammatory diseases. *Proc Natl Acad Sci USA*. 2013;110:3507–12.
 52. Mestas J, Hughes CCW. Of mice and not men: differences between mouse and human immunology. *J Immunol*. 2004;172(5):2731–8.
 53. Donnelly RP, Sheikh F, Dickensheets H, Savan R, Young HA, Walter MR. Interleukin-26: An IL-10-related cytokine produced by Th17 cells. *Cytokine Growth Factor Rev*. 2010;21:393–401.
 54. Lüthje F, Skovgaard K, Jensen HE, Jensen LK. The inflammatory response to bone infection – a review based on animal models and human patients. *APMIS*. 2020;128(4):275–86.
 55. Wada T, Nakashima T, Hiroshi N, Penninger JM. RANKL-RANK signaling in osteoclastogenesis and bone disease. *Trends Mol Med*. 2006;12:17–25.

56. Cao F, Zhou W, Liu G, Xia T, Liu M, Mi B, et al. Staphylococcus aureus peptidoglycan promotes osteoclastogenesis via TLR2-mediated activation of the NF- κ B/NFATc1 signalling pathway. *Am J Transl Res*. 2017;9:5022–30.
57. Claro T, Widaa A, O'Seaghda M, Miajlovic H, Foster TJ, O'Brien FJ, et al. Staphylococcus aureus protein A binds to osteoblasts and triggers signals that weaken bone in osteomyelitis. *PLoS One*. 2011;6:1–10.
58. Jin T, Zhu YL, Li J, Shi J, HeXQ DJ, et al. Staphylococcal protein A, panton-valentine leukocidin and coagulase aggravate the bone loss and bone destruction in osteomyelitis. *Cell Physiol Biochem*. 2013;32:322–33.
59. Montonen M, Li TF, Lukinmaa PL, Sakai E, Hukkanen M, Sukura A, et al. RANKL and cathepsin K in diffuse sclerosing osteomyelitis of the mandible. *J Oral Pathol Med*. 2006;35:620–5.
60. Dapunt U, Giese T, Lasitschka F, Lehner B, Ewerbeck V, Hänsch GM. Osteoclast generation and cytokine profile at prosthetic interfaces: a study on tissue of patients with aseptic loosening or implant-associated infections. *Eur J Inflamm*. 2014;12:147–59.
61. Cawston TE, Young DA. Proteinases involved in matrix turnover during cartilage and bone breakdown. *Cell Tissue Res*. 2010;339:221–35.
62. Jensen HE, Nielsen OL, Agerholm JS, Iburg T, Johansen LK, Johannesson E, et al. A non-traumatic Staphylococcus aureus osteomyelitis model in pigs. *In vivo*. 2010;24:257–64.
63. Jensen HE. Skeletsystemet. In: Leifsson PS, Nielsen OL, Agerholm JS, Iburg T, editors. *Kødkontrol - det patoanatomiske grundlag*. Frederiksberg: Biofolia; 2010. p. 483–545.
64. Jensen HE, Jensen B, Arnbjerg J, Aalbæk B. Chronic purulent osteomyelitis complicated by chondrosis at the costochondral junction of slaughter pigs. *Eur J Vet Pathol*. 1999;5:3–7.
65. Keith T. Bone and Joints. In: Maxie MG, editor. *Jubb, Kennedy and Palmer's Pathology of Domestic Animals*, vol. 1. St Louis, MO: Elsevier; 2007. p. 1–185.
66. Gardhouse S, Guzman DSM, Paul-Murphy J, Byrne BA, Hawkins MG. Bacterial isolates and antimicrobial susceptibilities from odontogenic abscesses in rabbits: 48 cases. *Vet Record*. 2017;181:538–44.
67. Laimore MD, Khanna C. Naturally occurring diseases in animals: contributions to translational medicine. *ILAR J*. 2014;55:1–3.
68. Hasman H, Moodley A, Guardabassi L, Stegger M, Skov RL, Aarestrup FM. spa type distribution in Staphylococcus aureus originating from pigs, cattle and poultry. *Vet Microbiol*. 2010;141:326–31.
69. Johansen LK, Koch J, Frees D, Aalbæk B, Nielsen OL, Leifsson PS, et al. Pathology and biofilm formation in a porcine model of staphylococcal osteomyelitis. *J Comp Path*. 2012;147:343–53.
70. Christiansen JG, Jensen HE, Johansen LK, Koch J, Koch J, Aalbæk B, et al. Porcine models of non-bacterial thrombotic endocarditis (NBTE) and infective endocarditis (IE) caused by Staphylococcus aureus: a preliminary study. *J Heart Valve Dis*. 2013;22:368–76.
71. Sung JM, Lloyd DH, Lindsay JA. Staphylococcus aureus host specificity: comparative genomics of human versus animal isolates by multi-strain microarray. *Microbiology*. 2008;154:1949–59.
72. Knudsen DJ, Frimodt-Møller N. Animal models in bacteriology. In: Schmidt A, Weber OF, editor. *Animal testing in infectiology*. New York: Krager; 2001. p. 1–14.
73. Aalbæk B, Jensen LK, Jensen HE, Olsen JE, Christensen H. Whole genome sequence of Staphylococcus aureus S54F9 isolated from a chronic disseminated porcine lung abscess and used in human infection models. *Genome Announc*. 2015;3:1.
74. Van der Vorst JR, Van Dam RM, Van Stiphout RS, van den Broek MA, Hollander IH, Kessels KG, et al. Virtual liver resection and volumetric analysis of the future liver remnant using open source image processing software. *World J Surg*. 2010;34:2426–33.
75. Franssen BB, Van Diest PJ, Schuurman AH, Kon M. Drilling K-wires, what about osteocytes? An experimental study in rabbits. *Arc Orthop Traum Surg*. 2007;128:3174–83.
76. Bori G, McNally M, Athanasou N. Histopathology in periprosthetic joint infections: When will the morphomolecular diagnosis be a reality? *BioMed Res Int*. 2018;2018:1–10.
77. Morgenstern M, Athanasou NA, Fergusson JY, Metsemakers WJ, Atkins B, McNally M. The value of quantitative histology in the diagnosis of fracture-related infection. *Bone Joint J*. 2018;100-B(7):966–72.
78. Morawietz L, Tiddens O, Mueller M, Tohtz S, Gansukh SJH, et al. Twenty three neutrophil granulocytes in 10 high power fields is the best histological threshold to differentiate between aseptic and septic endoprosthesis loosening. *Histopathology*. 2009;54:847–53.
79. Pandey R, Drakoulakis E, Athanasou NA. An assessment of the histological criteria used to diagnose infection in hip revision arthroplasty tissues. *J Clin Pathol*. 1999;52:118–32.
80. Feldman DS, Lonner JH, Desai P, Zuckerman JD. The role of intraoperative frozen sections in revision total joint arthroplasty. *J Bone J Surg Am*. 1995;77:1807–13.

81. Zimmerli W, Trampuz A. Biomaterial-associated infection: A perspective from the clinic. In: Moriarty TF, editor. Biomaterials associated infection: Immunological aspects and antimicrobial strategies. Cham: Springer Science+Business Media; 2013. p. 3–24.
82. Aggarwal VK, Higuera C, Deirmengian G, Parvizi J, Matthew AS. Swab cultures are not as effective as tissue cultures for diagnosis of periprosthetic joint infections. *Clin Orthop Relat Res.* 2013;471:3196–203.
83. Song Z, Borgwardt L, Høihy N, Hong W, Sørensen TS, Borgwardt A. Prosthesis infections after joint replacement: the possible role of bacterial biofilms. *Orthop Rev.* 2013;5:65–71.
84. Soerensen KE, Skovgaard K, Heegaard PM, Jensen HE, Nielsen OL, Leifsson PS, et al. The impact of *Staphylococcus aureus* concentration on development of pulmonary lesions and cytokine expression after intravenous inoculation of pigs. *Vet Pathol.* 2012;49:950–62.
85. Koschmieder R, Ritzerfeld W, Homeyer L. Gentamycinzusatz zum polymethylmethacrylat zur behandlung von Knocheninfektionen. *Z Orthop.* 1975;113:147–9.
86. Patterson AL, Galloway RH, Baumgartner JC, Barsoum IS. Development of chronic mandibular osteomyelitis in a miniswine model. *J Oral Maxillofac Surg.* 1993;51:1358–62.
87. Rink A, Santschi EM, Beattie CW. Normalized cDNA libraries from a porcine model of orthopedic implant-associated infection. *Mamm Genome.* 2001;13:198–205.
88. Krenn V, Morawietz L, Perino G, Kienapfel H, Ascherl R, Hassenpflug GJ, et al. Revised histopathological consensus classification of joint implant related pathology. *Pathol Res Pract.* 2014;210:779–86.
89. Larsen MO, Rolin B. Use of Göttingen minipig as a model of diabetes, with special focus on type 1 diabetes research. *ILAR J.* 2004;45:303–13.
90. Coenye T, Goeres D, Van Bambeke F, Bjarnsholt B. Should standardized susceptibility testing for microbial biofilms be introduced in clinical practice? *Clin Microbiol Infect.* 2018;24:570–2.
91. Coenye T, Nelis HJ. In vitro and in vivo model systems to study microbial biofilm formation. *J Microbiol Methods.* 2010;83:89–105.
92. Isling LK, Aalbæk B, Birck MM, Heegaard PMH, Leifsson PS. Host response to porcine strains of *Escherichia coli* in a novel pyelonephritis model. *J Comp Pathol.* 2011;144:257–68.
93. Levison DA, Reid R, Burt AD, Harrison DJ, Flemming S editors. *Muir's textbook of pathology.* London: Taylor & Francis Ltd; 2008.
94. Jensen HE, Gyllenstein J, Hofman C, Leifsson PS, Agerholm JA, Boye M, et al. Histologic and bacteriologic findings in valvular endocarditis of slaughter-age pigs. *J Vet Diagn Investig.* 2010;22:921–7.
95. Damjanov I, Linder J, editors. *Anderson's Pathology.* London: CRC Press; 1995.
96. Maxie MG, Newman SJ. Urinary system. In: Maxie MG, editor. *Jubb, Kennedy and Palmer's pathology of domestic animals, Vol. 2.* St. Louis: Elsevier Limited; 2007. p. 425–523.
97. Costerton W, Veeh T, Shirtliff M, Pasmore M, Post C, Ehrlich G. The application of biofilm science to the study and control of chronic bacterial infections. *J Clin Invest.* 2003;112:1466–77.
98. Donlan RM, Costerton JW. Biofilms: survival mechanisms of clinically relevant microorganisms. *Clin Microbiol Rev.* 2002;15:167–93.
99. Stoodley P, Nistico L, Johnson S, Lasko LA, Baratz M, Gahlot V, et al. Direct demonstration of viable *Staphylococcus aureus* biofilm in an infected total joint arthroplasty. A case-report. *J Bone J Surg Am.* 2008;90:1751–8.
100. Kirketerp-Møller K, Jensen P, Fazli M, Madsen KG, Pedersen J, Moser C, et al. Distribution, organization, and ecology of bacteria in chronic wounds. *J Clin Microbiol.* 2008;46:2717–22.
101. Bjarnsholt T, Jensen PØ, Fiandaca MJ, Pedersen J, Hansens CR, Andersen CB, et al. *Pseudomonas aeruginosa* biofilm in the respiratory tract of cystic fibrosis patients. *Pediatric Pulmonol.* 2009;44:547–58.
102. Boelens JJ, Zaat SAJ, Meeldijk J, Dankert J. Subcutaneous abscess formation around catheters induced by viable *S. epidermidis* as well as by small amounts of bacterial cell wall components. *J Biomed Mat Res.* 2000;50:546–56.
103. Boelens JJ, Zaat SAJ, Munk JL, Weening JJ, Van der Poll T, Dankert J. Enhanced susceptibility to subcutaneous abscess formation and persistent infection around catheters is associated with sustained interleukin-1-beta levels. *Infect Immun.* 2000;68:1692–5.
104. Costerton JW. Biofilm theory can guide the treatment of device related orthopaedic infections. *Clin orthop research.* 2005;437:7–11.
105. Tuchscher L, Kreis CA, Hoerr V, Flint L, Hachmeister M, Geraci J, et al. *Staphylococcus aureus* develops increased resistance to antibiotics by forming dynamic small colony variants during chronic osteomyelitis. *J Antimicrob Chemother.* 2016;71:438–48.
106. Valour F, Trouillet-Assant S, Riffard N, Tasse J, Flammier S, Raigade JP, et al. Antimicrobial activity against intraosteoblastic *Staphylococcus aureus*. *J Antimicrob Chemother.* 2015;59:2029–36.
107. Rumbaugh KP, Carty NL. In vivo models of biofilm infection. In: Bjarnsholt T, editor.

- Biofilm infections. New York: Springer-Verlag; 2011. p. 267–90.
108. Bancroft JD. Xxx. In: Bancroft JD, Gamble M, editors. *Theory and practice of histological techniques*. London: Churchill Livingstone Elsevier; 2008.
 109. Flemming H-C, Wingender J. The biofilm matrix. *Nature Rev Microbiol*. 2010;8:623–33.
 110. Johansen LK, Koch J, Kirketerp-Møller K, Wamsler OJ, Nielsen OL, Leifsson PS, et al. Therapy of haematogenous osteomyelitis: a comparative study in a porcine model and Angolan children. *In Vivo*. 2013;27:305–12.
 111. Høiby N, Bjarnsholt T, Moser C, Bassi GL, Coenye T, Donelli G, et al. ESCMID guideline for the diagnosis and treatment of biofilm infections 2014. *Clin Microbiol Infect*. 2015;21:1–25.
 112. Lee J, Kang CL, Lee JH, Joung M, Moon S, Wi YM, et al. Risk factors for treatment failure in patients with prosthetic joint infections. *J Hosp Infect*. 2010;75:273–6.
 113. Marculescu CE, Berbari EF, Hansen AD, Steckelberg JM, Harmsen SW, Mandrekar JN, et al. Outcome of prosthetic joint infections treated with debridement and retention of components. *Clin Infect Dis*. 2006;42:471–8.
 114. Drusano GL. Pharmacokinetics and pharmacodynamics of antimicrobials. *Clin Infect Dis*. 2007;45:89–95.
 115. Tøttrup M, Søballe K, Bibby BM, Forsingdal TH, Hansen P, et al. Bone, subcutaneous tissue and plasma pharmacokinetics of cefuroxime in total knee replacement patients – a randomized controlled trial comparing continuous and short-term infusion. *APMIS*. 2019;127:779–88.
 116. Bue M, Birke-Sørensen H, Thillemann TM, Hardlei TF, Søballe K, Tøttrup M. Single-dose pharmacokinetics of vancomycin in porcine cancellous and cortical bone determined by microdialysis. *Int J Antimicrob Agents*. 2015;46:434–8.
 117. Landersdorfer CB, Bulitta JB, Kinzig M, Holzgrabe U, Sörgel F. Penetration of antimicrobials into bone: pharmacokinetic, pharmacodynamic and bioanalytical considerations. *Clin Pharmacokinet*. 2009;48:89–124.
 118. Joukhadar C, Müller M. Microdialysis: current applications in clinical pharmacokinetic studies and its potential role in the future. *Clin Pharmacokinet*. 2005;44:895–913.
 119. Wagner C, Sauermann R, Joukhasar G. Principles of antibiotic penetration into abscess fluid. *Pharmacology*. 2006;78:1–10.
 120. Barza M, Cuchural G. General principles of antibiotic tissue penetration. *J Antimicrob Chemother*. 1985;15:59–75.
 121. Ferguson J, Diefenbeck M, McNally M. Ceramic biocomposites as biodegradable antibiotic carriers in the treatment of bone infections. *J Bone Joint Infect*. 2017;2:38–51.
 122. Walenkamp GH, Vree TOMB, Van Rens TJ. Gentamicin-PMMA beads: pharmacokinetic and nephrotoxicological study. *Clin Orthop Relat Res*. 1986;205:171–83.
 123. Stravinskas M, Horstmann PF, Ferguson J, Hettwer NM, Tarasevicius S, et al. Pharmacokinetics of gentamicin eluted from a regenerating bone graft substitute: in vitro and clinical release study. *Bone Joint Res*. 2016;5:427–35.
 124. Ter Boo GJ, Grijpma DW, Moriarty TF, Richards RG, Eglin D. Antimicrobial delivery systems for local infection prophylaxis in orthopaedic and trauma surgery. *Biomaterials*. 2015;52:113–25.
 125. McNally M, Ferguson J, Diefenbeck M, Lau A, Scarborough M, Ramsden A, et al. Single-stage treatment of chronic osteomyelitis with a new absorbable, gentamicin-loaded, calcium sulphate/hydroxyapatite biocomposite. A prospective series of 100 cases. *Bone Joint J*. 2016;98:1289–96.
 126. Ackermann MR. Inflammation and healing. In: Zachary JF, editor. *Pathologic basis of veterinary disease*. 6th ed., St Louis, MO: Elsevier; 2017. p. 954-1009.
 127. Baudoux P, Bles N, Lemaire S, Mingeot-Leclercq M-P, Tulkens PM, van Bambeke F. Combined effect of pH and concentration on the activities of gentamicin and oxacillin against *Staphylococcus aureus* in pharmacodynamic models of extracellular and intracellular infections. *J Antimicrob Chemother*. 2007;59:246–53.